energies

MDPI

Article

Energy and Exergy-Based Screening of Various Refrigerants, Hydrocarbons and Siloxanes for the Optimization of Biomass Boiler–Organic Rankine Cycle (BB–ORC) Heat and Power Cogeneration Plants

Savvas L. Douvartzides [1,*], Aristidis Tsiolikas [1,2], Nikolaos D. Charisiou [3], Manolis Souliotis [4], Vayos Karayannis [4] and Nikolaos Taousanidis [5]

1 Laboratory of Internal Combustion Engines, Department of Mechanical Engineering, University of Western Macedonia, 50100 Kozani, Greece; aristeidistsio@yahoo.com
2 Design and Manufacturing Laboratory, Department of Mechanical Engineering, University of Thessaly, 43100 Karditsa, Greece
3 Laboratory of Alternative Fuels and Environmental Catalysis, Department of Chemical Engineering, University of Western Macedonia, 50100 Kozani, Greece; ncharisiou@uowm.gr
4 Department of Chemical Engineering, University of Western Macedonia, 50100 Kozani, Greece; msouliotis@uowm.gr (M.S.); vkarayannis@uowm.gr (V.K.)
5 Centre of Renewable and Alternative Energy Forms and Rational Use of Energy, Department of Mechanical Engineering, University of Western Macedonia, 50100 Kozani, Greece; ntaousanidis@uowm.gr
* Correspondence: sdouvartzidis@uowm.gr

check for updates

Citation: Douvartzides, S.L.; Tsiolikas, A.; Charisiou, N.D.; Souliotis, M.; Karayannis, V.; Taousanidis, N. Energy and Exergy-Based Screening of Various Refrigerants, Hydrocarbons and Siloxanes for the Optimization of Biomass Boiler–Organic Rankine Cycle (BB–ORC) Heat and Power Cogeneration Plants. *Energies* **2022**, *15*, 5513. https://doi.org/10.3390/en15155513

Academic Editor: Andrea De Pascale

Received: 14 June 2022
Accepted: 25 July 2022
Published: 29 July 2022

Abstract: The cogeneration of power and heat was investigated for Biomass Boiler–Organic Rankine Cycle (BB–ORC) plants with the characteristics of typical units, such as the 1 MW_{el} Turboden ORC 10 CHP. The thermodynamic analysis of the ORC unit was undertaken considering forty-two (42) dry and isentropic candidate pure working fluids. Only subcritical Rankine cycles were considered, and the pinch point temperature differences for the evaporation and condensation heat exchangers were kept constant at 10 °C in all cases. The study provides an original and unique screening of almost all pure working fluids that are considered appropriate in the literature under the same operation and optimization conditions and compiles them into a single reference. In its conclusions, the study provides useful fluid selection and design guidelines, which may be easily followed depending on the optimization objective of the ORC designer or operator. In general, hydrocarbons are found to lie in the optimum middle range of the fluid spectrum, between the siloxanes that maximize the production of mechanical power and the refrigerants that maximize the production of heat. Specific hydrocarbon fluids, such as cyclopentane, heptane, hexane, benzene, and toluene, are found as rational options for maximum mechanical efficiency when operating with practically feasible condensation pressures between 10 and 200 kPa. At condensation pressures below 10 kPa, ethylbenzene, o-xylene, m-xylene, p-xylene, and nonane are also found to be feasible options. Finally, cyclopentane, hexane, and MM (hexamethyldisiloxane) are selected as the most appropriate options for cogeneration plants aiming simultaneously at high mechanical power and maximum temperature water production.

Keywords: biomass boiler; organic rankine cycle; thermodynamic analysis; dry and isentropic fluids; cogeneration of power and heat

1. Introduction

The continuous utilization of fossil fuels, such as coal, natural gas, gasoline, and diesel oil, is widely regarded as the main reason behind serious undesired phenomena, such as environmental pollution and global climate change. Worldwide, these side effects are nowadays being combated by gradually introducing into the energy market renewable

energy sources, such as solar, geothermal, and biomass [1–4]. Biomass, especially, is considered as an abundant energy resource that can play a significant role in the future energy supply, offering the advantages of renewability and a neutral CO_2 environmental impact. Biomass also facilitates the development of decentralized power generation plants with lower transmission and distribution costs and the installation of biomass-based electricity infrastructures, which can be easily integrated into the existing processing or power generating units without weather or time restrictions. Moreover, it can be converted into all major energy carriers, such as electricity, heat, and transport fuels, as well as into a wide variety of chemicals and materials that are traditionally produced from fossil fuels [5–8]. In 2010, solid biomass contributed about 90 TWh of electricity, but according to the IEA Bioenergy Roadmap, a threefold increase is expected by 2025 [9]. The main technology for the production of heat and power from biomass is combustion, but efficiency can be enhanced by the combined generation of heat and power by conventional technologies or by the combination of biomass combustion with Organic Rankine Cycles (ORCs) [10,11].

During the last decades, the technology of the ORCs has reached the level of maturity required for the efficient exploitation of low-grade thermal energy in both waste heat recovery and combined heat and power (CHP) cogeneration applications. ORCs operate similarly to the conventional steam Rankine power cycles, but water is replaced by an appropriate organic working fluid with suitable thermodynamic and physicochemical characteristics for the optimization of the efficiency of the application when the temperature of the available heat source is medium or low. Such medium- and low-grade heat sources include concentrating solar energy [12–18], geothermal fields [14–16,19], and waste heat rejected by industrial processes and combined cycles [14–16,20–22] or by biomass-fired plants [14–16,23–30]. Specifically for biomass-fired plants, Pantaleo et al. [23] proposed a thermoeconomic analysis of small-scale CHP plants based on a steam turbine or an externally fired micro gas turbine coupled to different typologies of bottoming ORC. Qiu et al. [24] presented an experimental investigation on the biomass-fired organic Rankine cycle (ORC)-based micro-CHP and showed that it could generate 861 W of electricity and 47.26 kW_{th} of heat, corresponding to an electricity generation efficiency of 1.41% and a CHP efficiency of 78.69%. Nur et al. [26] investigated the thermodynamic performance of a small biomass-fueled ORC plant for the generation of electricity, using fuel wastes from the operation of palm oil mills. Algieri and Morrone [27] studied the energetic performances and the economic feasibility of ORCs for biomass single-family CHP generation, carrying out a parametric energy analysis to identify the appropriate system configurations. Zhu et al. [28] carried out an interesting study regarding the design of a biomass-fired ORC–CHP system, integrated with monoethanolamine-based CO_2 capture. The authors assumed that the pressurized hot water would be used as a heat source for the ORC system and that the condensation heat would be fully utilized to supply domestic hot water. Eyidogan et al. [29] provided a survey in relation to the technical and economic analyses of ORC systems in Turkey and their application areas. Finally, Imran et al. [30] used a bibliometric approach to analyze the scientific publications regarding the organic Rankine cycle in the period 2000–2016, concluding that China, the United States, Italy, Greece, Belgium, Spain, Germany, and the United Kingdom are the leading countries in the field, as they account for 64% of the total number of publications. The authors also concluded that the core research activities are focused on applications of the organic Rankine cycle technology, working fluids selection/performance, cycle architecture, and design/optimization.

ORC technology is especially suitable in plants operating with biomass where it can provide heat and power in production-dedicated facilities, such as sawmills, pellet factories, and medium density fiberboards (MDFs) or particleboard production plants. Biomass has low energy density, which increases the transport costs, and most of these facilities usually have increased demands for electricity and heat or cold. Electricity may be used to cover the internal energy needs of the plant, and heat may find application for the processing of materials (drying, etc.) in endothermic chemical reactions, in the production of hot water, or in space and district heating. According to a study of Tartiére and Astolfi [31],

the global installed capacity of biomass-fired ORC plants in 2016 was about 301 MW with about 332 plants around the world. More than 228 of these plants were built by the Italian company Turboden, and most of them operate for CHP applications of a power output of up to 2.5 MW, although CHP units with electrical capacities up to 30 MW are also commercially available [32]. All these plants may be referred to as Biomass Boiler–Organic Rankine Cycle (BB–ORC) systems and consist of a biomass-fed boiler and an ORC module coupled via a thermal oil loop. Biomass is fired in a grate furnace, and the thermal oil serves as a heat transfer medium between the combustion gases and the organic fluid of the ORC module. The utilization of the thermal oil provides a number of technical advantages including low pressure in the boiler, sensitivity to load changes, and simple and safe control and operation. In addition, the maximum temperature of a biomass system is significantly higher than in other ORC applications reaching values up to 400 °C. The thermal oil is necessary to avoid the excessive heating of the organic fluid, which above a critical temperature becomes chemically unstable [33]. For the majority of the organic fluids, this temperature upper limit may be considered about 350 °C. Schuster et al. [34] argued that the technology of the ORCs is only reliable for decentralized power plants fed by solid fuels, such as biomass, with an electrical power output up to 1 MW.

The optimization of a BB–ORC unit depends largely on the selection of the appropriate ORC working fluid. This can take place among a variety of hydrochlorofluorocarbons, hydrofluorocarbons, perfluorocarbons, hydrocarbons, and siloxanes. In most commercial biomass-fired plants, siloxane or cyclopentane is used [35]. Siloxanes perform well in low-grade heat applications, such as in geothermal and low-temperature waste heat units, but result in low efficiencies in higher grade heat applications, such as in biomass-fired or gas turbine bottoming cycles. In response, various studies focused on the screening of alternative organic fluids with interesting results. Drescher and Brüggemann [36] have reported that toluene and various alkylbenzenes, such as ethylbenzene, propylbenzene, and butylbenzene, can provide higher efficiencies than MDM (octamethyltrisiloxane or OMTS). Ismail et al. [37] compared eight organic fluids (toluene, cyclohexane, decane, dodecane, propylcyclohexane, MDM, nonane, and R113) and four ORC design scenarios with or without internal regeneration and with saturated vapor or superheated vapor at the inlet of the turbine. Toluene was found to be the best fluid when regeneration is not used; dodecane was found to be the best with regeneration and saturated vapor, and propylcyclohexane was selected with regeneration and superheating. Algieri [38] investigated cyclohexane, decane, and toluene as working fluids in a biomass-fired ORC heat and power cogeneration system and concluded that higher electrical efficiency is achieved with toluene and internal regeneration, while higher thermal efficiency is provided by decane. Toluene was selected also by Pezzuolo et al. [39] as the best choice for regenerative cycles among other fluids, such as o-xylene, p-xylene, m-xylene, and ethylbenzene. Jang and Lee [40] examined three groups of fluids for a BB–ORC heat and power cogeneration system with an electrical output of 2 kW and a thermal output of 25 kW. The first group included hydrocarbon fluids, such as cyclopentane, isopentane, n-pentane, and diethyl ether; the second group included R1233zd and R245fa, and the third group included HFE-7000 and HFE-7100. Their results have shown that the first group of hydrocarbon fluids provides higher ORC and CHP efficiency and lower fluid mass flow rates, which imply smaller pumps and a more compact plant design. Lower CHP efficiency and higher mass flow rates were those of the third group of fluids. Mikielewicz and Mikielewicz [41] examined several organic fluids, such as heptane, pentane, R123, R365mfc, R141b, and ethanol and confirmed that R141b and ethanol are excellent fluids. R141b was also selected for biomass-fired ORC's by Moharamian et al. [42] as it was observed to provide the highest energy and exergy efficiencies among the examined fluids in the order R141b > R123 > n-pentane > water > HFE7000. Finally, various siloxanes have been examined for high-temperature ORC applications by Fernández et al. [43]. They concluded that simple linear siloxanes, MM (hexamethyldisiloxane), and MDM (octamethyltrisiloxane) are highly efficient and thermally stable, and they comment that more complex siloxanes, such as D5 (decamethylcyclopentasiloxane), D6

(dodecamethylcyclohexasiloxane), and MD2M (decamethyltetrasiloxane), are characterized by low condensing pressure.

Recently, Méndez-Cruz et al. [44] presented a methodology to evaluate the feasibility of using a refrigerant as a working fluid in an organic Rankine cycle based on an exergetic viability index. As a case study, R134a, R600a, R245fa, and R123 refrigerants were considered. Thurairaja et al. [45] focused their research on the performance evaluation of ORCs for different working fluids. The modeling work was performed using MATLAB and a thermophysical database, REFPROP. The evaluation was performed based on the performance of the working fluid. The results revealed that MD2M and cyclopentane for temperature ranges 50–100 °C; butane, neopentane, and R245fa for 100–150 °C; ethanol, methanol, and propanone for 150–200 °C; water, m-Xylene, and p-Xylene for 200–320 °C were better working fluids for energy extraction. Babatunde and Sunday [46] reviewed the working fluids for different applications, and they concluded that the thermophysical properties along with the stability and the environmental effects are essential factors to be considered when making a choice of the most appropriate working fluid.

The main objective of the study of Arjunan et al. [47] was to identify the most suitable organic fluids having the characteristics necessary for use in solar ORCs. In addition, a detailed review of the various types of heat transfer fluids available in the market that were often used in ORC systems was conducted. They concluded that below 250 °C, R245fa, R134a, carbon dioxide, n-butane, i-butane, and propane are usually preferred. In addition, above 350 °C, water and toluene have better utility. R12, R113, R114, and RC318 are examples of fluids having high ODP and GWP values. These were not chosen owing to environmental factors. Several fluids, such as R141b, R123, R134a, and R32 have low GWP and low ODP values.

Imre et al. [48] proposed a novel method to choose the optimal working fluid—solely from the point of view of the expansion route—for a given heat source and heat sink (characterized by a maximum and minimum temperature). The basis of this method was the novel classification of working fluids using the sequences of their characteristic points on temperature–entropy space. Zhang et al. [49] claimed that the expander is a key device in ORC. Through calculation and analysis, an ORC system that uses a single-screw expander and undergoes a vapor–liquid two-phase expansion is able to obtain higher thermal efficiency, higher net work output, and smaller heat exchange load of the condenser. Finally, Invernizzi et al. [50] investigated the use of pure and hydrocarbon binary mixtures as potential alternative working fluids in a usual biomass-powered ORC. A typical biomass combined heat and power plant installed in Cremona (Italy) was considered as the benchmark. Among the many conceivable different mixtures of hydrocarbons, they identified mixtures of iso-octane and n-octane. These mixtures had modest temperature "glides" at every composition, and the corresponding mixture critical temperature results were always greater than the maximum assumed working temperature at 260 °C.

Despite the extensive research on pure working fluids for various ORCs, as discussed above, these results are dispersed in various literature sources and correspond to quite different ORC operation conditions. Therefore, the designer of such plants and systems lacks a practical guide, which compares all the pure fluid options in a systematic way, under the same operation and optimization conditions and compiles them into a single piece of literature. The present work comes as a response to this necessity and provides an original thermodynamic and technical comparison of almost all pure working fluids used in BB–ORC or waste heat recovery applications. The operation conditions of the BB–ORC plant are the same for all the fluids examined and similar to those reported for relevant commercial units, such as the 1 MW_{el} Turboden ORC 10 CHP.

2. The ORC–CHP System and the Working Fluids

An ORC system operates according to a closed Rankine thermodynamic cycle having as a working medium a suitable organic fluid. The T-s diagram of the cycle and the relevant system layout are shown in Figure 1.

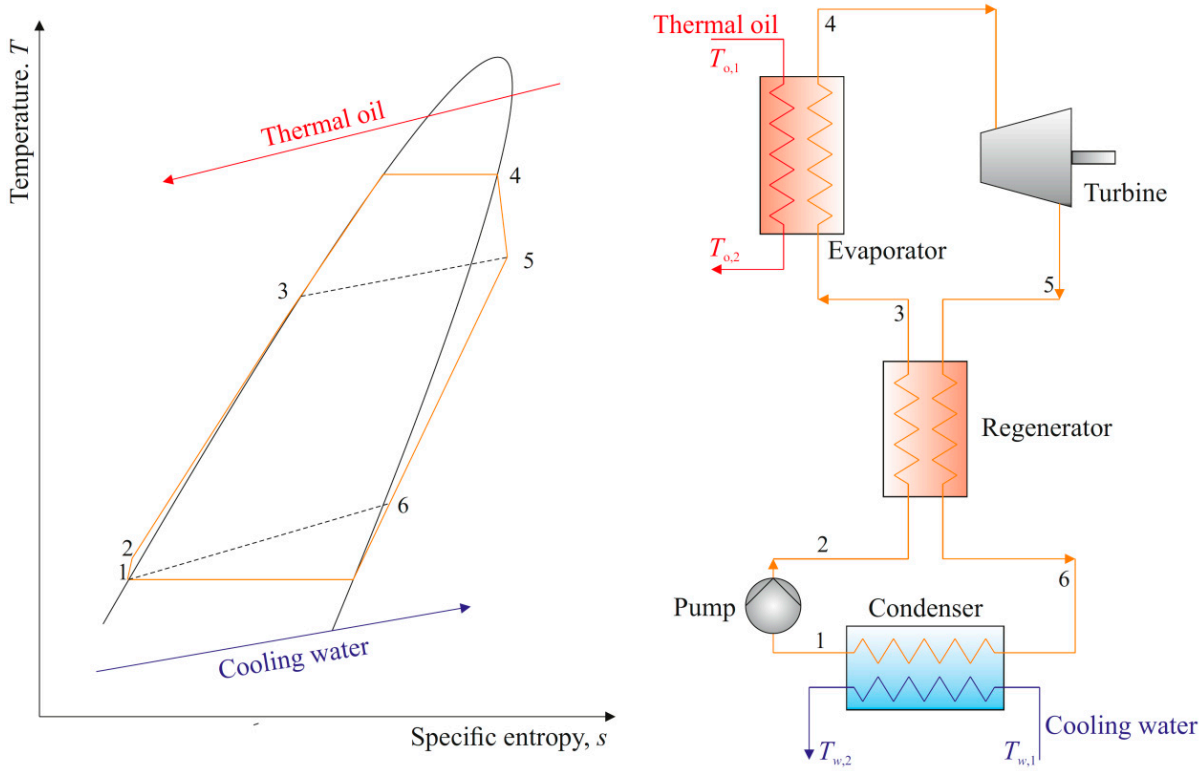

Figure 1. T-s diagram and system layout of the ORC–CHP unit.

A detailed presentation of the processes comprising the closed cycle is as follows:

i. Process 1–2: compression of liquid organic fluid in a pump.
ii. Process 2–3: isobaric preheating of the organic fluid in a vapor to liquid heat exchanger termed as recuperator or regenerator.
iii. Process 3–4: isobaric heat addition and evaporation of the organic fluid in an oil heat recovery exchanger. Evaporation may take place at a pressure higher or lower than the critical pressure of the working fluid, but in the present study, only subcritical pressures will be considered.
iv. Process 4–5: expansion of the organic fluid in a turbine (expander).
v. Process 5–6: isobaric cooling of the organic fluid in the regenerator.
vi. Process 6–1: isobaric cooling of the organic fluid and condensation to the state of saturated liquid 1 (also heating of the process water flow).

When operating with an appropriate working fluid, these ORC systems exhibit high cycle efficiency and very long operational life due to the noneroding and noncorroding fluid behavior on the system components, such as the turbine blades, tubing, and valves. Significant other advantages are the high turbine efficiency, the low turbine stresses, and the absence of turbine to electrical generator gear reduction due to turbine operation at low speeds. The system operation is also quiet and requires minimal maintenance.

The present study focuses on a BB–ORC heat and an electrical power cogeneration plant, similar to commercially available units, such as the Turboden 10 CHP. For this commercial unit, the manufacturer claims a gross electrical output of 1 MW_{el}, and the operational characteristics are shown in Table 1 [32].

Table 1. Performance characteristics of the 1 MW_{el} Turboden ORC 10 CHP commercial unit.

Overall thermal power input	$\dot{Q}_{in} = 5140$ kW
Biomass consumption [1]	2471 kg/h
Gross active electric power (turbine power)	$\dot{W}_{el} = 1000$ kW
Thermal power to hot water circuit	4081 kW
Gross electric efficiency	19.8%
Thermal efficiency for water heating	79.4%
Thermal oil inlet temperature	$T_{o,1} = 300$ °C
Thermal oil outlet temperature	$T_{o,2} = 240$ °C
Cooling water inlet temperature	$T_{w,1} = 60$ °C
Cooling water outlet temperature	$T_{w,2} = 80$ °C

[1] Assuming a low heating value of biomass LHV = 9.36 MJ/kg and the effectiveness of the evaporator is equal to 80%.

2.1. Classification of the Working Fluids according to Chemical Structure

The selection of the working fluid is of key importance for the thermal performance of ORC systems. The working fluids may be classified according to their chemical structure into chlorofluorocarbons (CFCs), hydrochlorofluorocarbons (HCFCs), hydrofluorocarbons (HFCs), perfluorocarbons (PFCs), hydrolfluoroolefins (HFOs), hydrocarbons (HCs), siloxanes, and other fluids, such as water. Table 2 presents this classification giving typical dry and isentropic working fluids for each chemical class together with their physical properties, such as their molecular weight MW and their critical temperature T_{cr} and critical pressure p_{cr}. Despite the fact that some hydrocarbons find application as refrigerants, the current study will assume all hydrocarbons as a separate class due to their specific chemical structure by only hydrogen and carbon atoms.

Uusitalo et al. [51] have reported a set of general recommendations for the design of ORCs summarized as follows:

(a) hydrocarbons can provide high efficiencies when they have a high critical temperature and high molar mass;
(b) they provide a higher enthalpy drop in the expander in comparison to siloxanes of the same critical temperature;
(c) cycloalkanes are more efficient than linear hydrocarbons of the same critical temperature;
(d) siloxanes can provide high efficiencies with high expander inlet temperatures in cycles equipped with a regenerator;
(e) they have a similar performance independent of their cyclic or linear molecular structure if they have the same critical pressure;
(f) fluorocarbons have lower cycle efficiencies compared to siloxanes and hydrocarbons, especially in high temperature processes;
(g) they provide lower enthalpy drop in the expander compared to hydrocarbons.

Table 2. Thermodynamic properties, environmental parameters, and safety classification of various fluids (n.a.: not available).

Code	Substance Name	MW (kg/kmol)	Latent heat of Vaporization ΔH_{vap} at 0.1 Mpa (kJ/kg)	Critical Temperature T_{cr} (K)	Critical Pressure p_{cr} (Mpa)	Type of Fluid	Ozone Depletion Potential (ODP)	Global Warming Potential (GWP) 100 y	ASHRAE 34 Safety Group
Chlorofluorocarbons (CFCs)									
R11	Trichloromonofluoromethane	137.37	181.49	471.11	4.4076	Isentropic	1	4750	A1
R113	1,1,2-Trichloro-1,2,2-Trifluoroethane	187.38	144.45	487.21	3.3922	Dry	1	6130	A1
R114	1,2-Dichloro-1,1,2,2-Tetrafluoroethane	170.92	136.06	418.83	3.257	Dry	1	10,000	A1

Table 2. *Cont.*

Code	Substance Name	MW (kg/kmol)	Latent heat of Vaporization ΔH_{vap} at 0.1 Mpa (kJ/kg)	Critical Temperature T_{cr} (K)	Critical Pressure p_{cr} (Mpa)	Type of Fluid	Ozone Depletion Potential (ODP)	Global Warming Potential (GWP) 100 y	ASHRAE 34 Safety Group
				Hydrochlorofluorocarbons (HCFCs)					
R123	2,2-Dichloro-1,1,1-Trifluoroethane	152.93	170.35	456.831	3.6618	Dry	0.02	77	B1
R124	1-Chloro-1,2,2,2-Tetrafluoroethane	136.5	165.99	395.425	3.6242	Isentropic	0.022	609	A1
R141b	1,1-Dichloro-1-Fluoroethane	116.9	222.88	477.5	4.212	Isentropic	0.12	725	A2
R142b	1-Chloro-1,1-Difluoroethane	100.5	223.43	410.26	4.055	Isentropic	0.12	2310	A2
				Hydrofluorocarbons (HFCs)					
R125	Pentafluoroethane	120	164.25	339.173	3.6177	Isentropic	0	3500	A1
R227ea	1,1,1,2,3,3,3-Heptafluoropropane	170.02	131.90	374.9	2.92	Dry	0	3220	A1
R236ea	1,1,1,2,3,3-Hexafluoropropane	152	165.32	412.44	3.5019	Dry	0	1370	n.a.
R236fa	1,1,1,3,3,3-Hexafluoropropane	152	160.48	398.07	3.2	Dry	0	9810	A1
R245ca	1,1,2,2,3-Pentafluoropropane	134	201.15	447.57	3.925	Dry	0	693	n.a.
R245fa	1,1,1,3,3-Pentafluoropropane	134	196.88	427.2	3.64	Dry	0	1030	B1
R365mfc	1,1,1,3,3-Pentafluorobutane	148.07	188.36	460.0	3.26	Dry	0	796	n.a.
				Perfluorocarbons (PFCs)					
R116	Hexafluoroethane	138.02	117.09	293.03	3.048	Isentropic	0	12,200	A1
RC318	Octafluorocyclobutane	200.03	116.87	388.38	2.77	Dry	0	10,300	A1
				Hydrofluoroolefins (HFOs)					
R1233zd(E)	trans-1-chloro-3,3,3-trifluoro-1-propene	130.49	195.52	439.6	3.62	Isentropic	0	74	A1
R1234yf	2,3,3,3-Tetrafluoropropene	114.04	180.40	367.85	3.38	Dry	0	4	A2L
R1234ze(E)	trans-1,3,3,3-Tetrafluoropropene	114.04	195.60	382.52	3.63	Isentropic	n.a.	6	n.a.
R1234ze(Z)	1,3,3,3-Tetrafluoropropene	114.04	215.11	423.27	3.53	Isentropic	n.a.	1.4	n.a.
				Hydrocarbons (HCs)					
R601	n-Pentane	72.1	357.89	469.7	3.37	Dry	0	4	A3
R601a	Isopentane	72.14	343.57	460.35	3.37	Dry	0	4	A3
	Cyclopentane	70.13	389.45	511.72	4.57	Dry	0	11	n.a.
	Neo-Pentane	72.14	315.95	433.74	3.19	Dry	0	n.a.	A3
	n-Hexane	86.17	335.24	507.82	3.03	Dry	n.a.	n.a.	n.a.
	Cyclohexane	84.15	356.66	553.64	4.07	Dry	n.a.	n.a.	A3
	n-Heptane	100.20	317.20	540.13	2.73	Dry	n.a.	n.a.	n.a.
	n-Nonane	128.25	288.91	594.55	2.28	Dry	n.a.	n.a.	n.a.
	n-Decane	142.28	276.72	617.7	2.10	Dry	n.a.	n.a.	n.a.
	Benzene	78.11	394.96	562.02	4.89	Dry	n.a.	n.a.	B2
	Ethyl Benzene	106.16	335.60	617.12	3.62	Dry	n.a.	n.a.	n.a.
	Toluene	92.13	361.00	591.75	4.12	Dry	n.a.	n.a.	A3
	m-Hylene	106.16	340.44	616.89	3.53	Dry	n.a.	n.a.	n.a.
	o-Hylene	160.16	343.01	630.25	3.73	Dry	n.a.	n.a.	n.a.
	p-Hylene	106.16	336.66	616.16	3.53	Dry	n.a.	n.a.	n.a.
				Siloxanes					
	D4	296.61	131.23	586.5	1.34	Dry	n.a.	n.a.	A3
	D5	370.76	111.72	619.15	1.16	Dry	n.a.	n.a.	n.a.
	D6	444.92	99.23	645.78	0.96	Dry	n.a.	n.a.	n.a.
	MD2M	310.68	129.22	599.4	1.22	Dry	n.a.	n.a.	A3
	MD3M	384.83	110.84	628.3	0.94	Dry	n.a.	n.a.	n.a.
	MDM (or OMTS)	236.65	152.78	564.09	1.41	Dry	n.a.	n.a.	n.a.
	MM	162.37	193.58	518.75	1.93	Dry	n.a.	n.a.	n.a.

2.2. Classification of Working Fluids according to the Slope of the Saturation Vapor Curve

The working fluids of the ORC cycles are also classified into three categories: wet fluids, dry fluids, and isentropic fluids. This classification is based on the sign of the following parameter ξ:

$$\xi = \frac{C_p}{T_{vap}} - \frac{\frac{nT_r}{1-T_r} + 1}{T_{vap}^2} \Delta H_{vap} \quad (1)$$

which represents the slope of the saturation curve of the vapor state of the organic fluid in a *T-s* diagram [52], as shown in Figure 2.

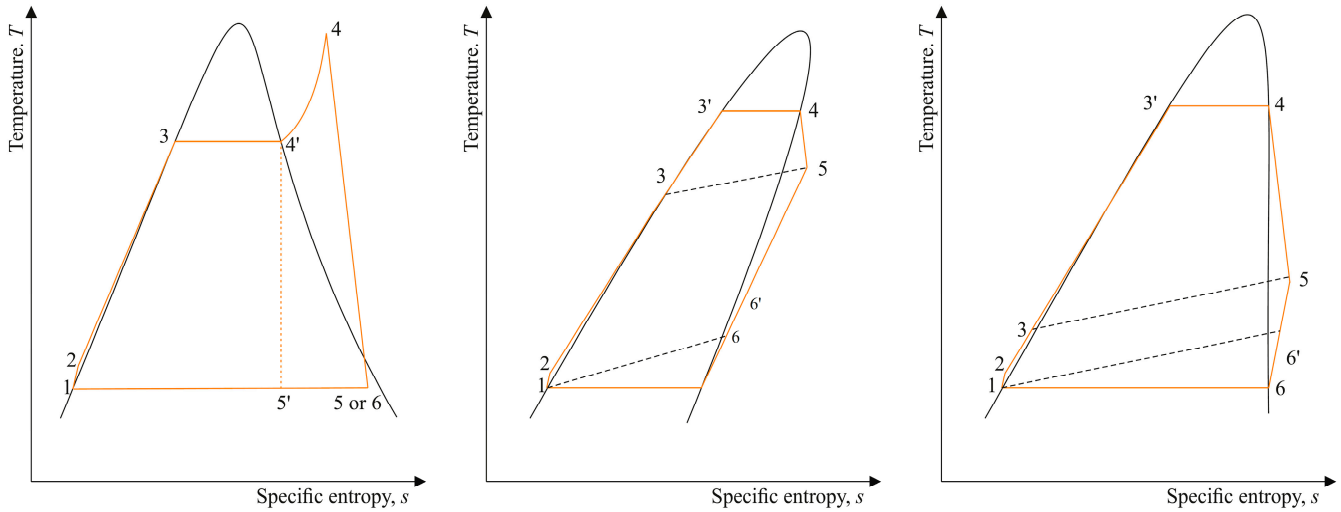

a) Wet fluids b) Dry fluids c) Isentropic fluids

Figure 2. (**a**) Typical organic Rankine cycles for wet fluids. Cycle 1-2-3-4′-5′-1 is the saturated Rankine cycle leading to high erosion of turbine blades due to the high liquid content of the saturated mixture of the expanded fluid at the state 5′. As a remedy, superheating 4′-4 is used, and the superheating wet fluid cycle 1-2-3-4-5-1- is generally used. Both these cycles usually do not use a regenerator. (**b**) Typical saturated organic Rankine of dry fluids. After expansion in the turbine, the fluid is in the high temperature superheating state 5. Regeneration 5–6 is used to exploit this energy and to increase the cycle efficiency by preheating the fluid exiting the pump in the process 2–3. (**c**) Typical saturated organic Rankine of isentropic fluids. Regeneration is possible as in the case of dry fluids [52].

In Equation (1), C_p is the specific heat of the fluid at constant pressure; T_{vap} is the evaporation temperature of the fluid; T_r is the reduced evaporation temperature ($T_r = T_{vap}/T_{cr}$, where T_{cr} is the critical temperature); ΔH_{vap} is the latent heat of vaporization, and n is 0.375 or 0.385 as suggested in [53]. Fluids with $\xi < 0$ are classified as wet; fluids with $\xi > 0$ are classified as dry, and fluids with $\xi \approx 0$ have an almost vertical saturation vapor curve and are classified as isentropic. This classification is shown schematically on the *T-s* diagrams of Figure 2 and is provided for each fluid in Table 2.

Conventional Rankine power plants use water as a working fluid, which is a wet fluid. Water is chemically stable, abundant, cheap, nontoxic, and environmentally friendly, but as all wet fluids, it is suitable only when superheating is applied to avoid the impingent of liquid water on the turbine blades, which causes erosion and wear. In addition, steam turbines are expensive and complex since they operate with large steam volumes. Due to these disadvantages, water and other wet fluids are suitable only for high-temperature applications, such as in plants for central power generation. In the ORC applications where low-grade heat is used, dry or isentropic fluids are generally suggested.

By using dry or isentropic fluids, wear of the turbine blades is avoided, but since the expanded vapor leaves the turbine with a high superheating enthalpy, a regeneration heat exchanger is usually used to absorb heat from the expanded vapor in order to preheat the

liquid fluid before the evaporator (Figures 1 and 2b,c). The regeneration equipment adds an extra investment cost for the ORC plant but rationalizes its energy management and reduces the operational costs by improving the achieved energy efficiency.

2.3. Environmental and Safety Selection Criteria

The optimal fluid for an ORC application must comply with a set of specific environmental and safety criteria. The environmental impact of each fluid is quantified using specific indices that measure the effect of fluid on the depletion of the atmospheric ozone layer and global warming. These indices are the Ozone Depletion Potential (ODP) and the Global Warming Potential (GWP), which are defined as follows [54]:

- Ozone Depletion Potential (ODP) quantifies the effect of each fluid on the degradation of the atmospheric ozone layer in comparison to the same effect of the specific fluid R11 for which it is considered that ODP equals unity (ODP = 1). The higher the ODP index of a fluid, the higher its impact on the ozone layer. Fluids with ODP below unity are considered to have an impact of medium intensity, and fluids with ODP above unity are considered highly detrimental to the ozone layer.
- Global Warming Potential (GWP) quantifies the solar heat absorbed by the gases of each fluid when released into the atmosphere in comparison to the solar heat absorbed by an equal mass of atmospheric carbon dioxide. Usually, GWP values are calculated over the time interval of 100 years and are considered low when GWP < 150, medium when 150 < GWP < 2500, and high when GWP > 2500.

The ODP index and GWP index for each specific working fluid is provided in Table 2.

The safety of a fluid for handling and during operation is estimated according to the ASHRAE 34 safety classification standard that classifies the substances into two health effect groups, A and B, and into three flammability groups, 1, 2, and 3. The criteria for these classification groups are as follows:

- Health group A indicates that the substance does not show any evidence of toxicity below 400 ppm.
- Health group B indicates that the substance shows evidence of toxicity below 400 ppm.
- Flammability group 1 indicates a fluid that does not propagate a flame in open air under normal conditions.
- Flammability group 2 indicates a fluid that may propagate a flame in open air under specific conditions.
- Flammability group 3 indicates a fluid of high flammability.
- Health and flammability classification groups are combined into a single safety classification index, which can be either A1, A2, A3, B1, B2, or B3. Recently, two new safety classes, A2L and B2L, were introduced for fluids that are mildly flammable. Table 2 provides the safety classification index for each specific working fluid.

Most of the chlorofluorocarbons, hydrochlorofluorocabons, hydrofluorocarbons, and perfluorocabons in Table 2 bear the symbol R in their code name due to their extensive utilization as refrigerants. Most of these fluids fall into the ASHRAE classification group A1 and are safe during handling and operation but leave to different extents a footprint on the environment, ozone, or climate. In 1987, the Montreal Protocol banned the utilization of CFCs due to their severe impact on the ozone layer. These were replaced by HCFCs, but their extensive use was soon recognized as a threat to the global climate. As a result, various analysts foresaw the gradual phase-out of HCFCs in the next years. Today, hydrofluorocabons are preferably selected having ODP indices equal to zero, but since their GWP indices are high, they are considered as contributors to the greenhouse effect and are considered also for gradual substitution in the future. Perfluorocarbons were also used as substitutes of CFCs but also contribute to global warming.

Hydrocarbons, such as pentane (R601), cyclopentane, cyclohexane, benzene, and toluene may also be considered as ORC working fluids, usually with a better thermodynamic performance than HFCs or HCFCs. As shown in Table 2, HCs have no impact on the

ozone layer or climate change but are highly flammable and need handling according to specific safety regulations and standards.

3. Modeling of the ORC–CHP Plant

The ORC–CHP plant was modeled assuming operation conditions similar to the Turboden unit described in Table 1. These are summarized in Table 3. As shown, the regenerator and the condenser were considered to have an efficiency of 80 %; the thermal oil inlet temperature was assumed equal to 350 °C, and the cooling water inlet temperature was assumed to be 30 °C. The modeling procedure requires the calculation of the thermodynamic properties of the states 1, 2, 3, 4′, 4, 5, 5′, and 6 shown in the *T-s* diagrams of Figure 2. Except temperature and pressure, other properties required for the analysis are specific enthalpy h, specific entropy s, and specific volume v. Two of the mentioned properties suffice for the calculation of all the others in a given state of the fluid. The properties of each fluid in the states of saturated liquid, saturated vapor, and superheated vapor were obtained by the open source thermodynamic package CoolProp [55].

Table 3. Assumed modeling parameters of the ORC plant [1].

Operation Parameter	Value
Thermal oil inlet temperature:	$T_{o,1} = 350$ °C
Cooling water inlet temperature:	$T_{w,1} = 30$ °C
Thermal oil flow rate:	$\dot{m}_o = 14$ kg/s
Cooling water flow rate:	$\dot{m}_w = 50$ kg/s
Thermal oil specific heat capacity:	$c_o = 2.3$ kJ/kgK
Cooling water specific heat capacity:	$c_w = 4.18$ kJ/kgK
Regenerator efficiency:	$\varepsilon_R = 0.8$ or $\varepsilon_R = 0$
Condenser efficiency:	$\varepsilon_C = 0.8$
Isentropic efficiency of pump:	$\eta_p = 0.85$
Isentropic efficiency of turbine (expander):	$\eta_t = 0.85$
Pinch point temperature difference in the evaporator:	$\Delta T_{pp} = 10$ °C
Pinch point temperature difference in the condenser:	$\Delta T_{pp} = 10$ °C

[1] Assuming a low heating value of biomass LHV = 9.36 MJ/kg and the effectiveness of the evaporator is equal to 80%.

The isentropic efficiencies of the pump η_p and the turbine η_t were assumed equal to 85%. The isentropic efficiency of the pump is defined as:

$$\eta_p = \frac{w_{ps}}{w_{pa}} = \frac{h_{2s} - h_1}{h_2 - h_1} \tag{2}$$

where w_{ps} is the ideal isentropic-specific pump work; w_{pa} is the actual nonisentropic specific pump work; h_1 is the specific enthalpy of the saturated liquid at the inlet of the pump; h_2 is the specific enthalpy of the compressed liquid at the exit of the actual pump, and h_{2s} is the specific enthalpy of the compressed liquid at the exit of the ideal isentropic pump. The isentropic efficiency of the turbine is defined as:

$$\eta_t = \frac{w_{ta}}{w_{ts}} = \frac{h_4 - h_5}{h_4 - h_{5s}} \tag{3}$$

where w_{ta} is the actual nonisentropic specific turbine work; w_{ts} is the ideal isentropic specific turbine work; h_4 is the specific enthalpy of the fluid vapor at the inlet of the turbine; h_5 is the specific enthalpy of the expanded fluid at the exit of the actual turbine, and h_{5s} is the specific enthalpy of the expanded fluid at the exit of the ideal isentropic turbine.

Process 1–2 is carried out by a pump that receives the working fluid in the state of saturated liquid at the pressure of the condenser and compresses it to the pressure of the isobaric evaporator. The actual specific work of the pump is calculated as:

$$w_{pa} = \frac{w_{ps}}{\eta_p} = \frac{v_1(P_2 - P_1)}{\eta_p} \tag{4}$$

where w_{ps} is the ideal (isentropic) work of the pump; v_1 is the specific volume of the saturated liquid fluid at the inlet of the pump; P_1 is the pressure of the condenser, and $P_2 = P_{vap}$ is the pressure of the evaporator. When regeneration is feasible, heat is recovered from the exhaust stream of the turbine inside the insulated isobaric regenerator. This results in the preheating of the working fluid before the evaporator, improving plant efficiency and biomass consumption. The efficiency of the regenerator was taken as $\varepsilon_R = 0.80$ when regeneration is employed and $\varepsilon_R = 0$ when regeneration is not used. The efficiency ε_R relates to the specific enthalpies in the inlet and outlet stream of the regenerator as:

$$\varepsilon_R = \frac{h_3 - h_2}{h_5 - h_6} \tag{5}$$

This expression enables the calculation of the specific enthalpy h_3 in the outlet of the regenerator. When regeneration is impossible and $\varepsilon_R = 0$, it is obviously valid $h_3 = h_2$.

The practical optimization of the ORC cycle equipment is of paramount importance since it maximizes heat recovery and system efficiency. The thermal design of the evaporator and the condenser in particular is known to be crucial in terms of both thermodynamic performance and cost. In this respect, the pinch point analysis is frequently used as a preliminary method for the selection of optimal cycle parameters [56–59]. Assuming a heat exchanger, such as the evaporator or the condenser, its hot and cold streams interact due to their local temperature difference. This must be positive in the entire flow field inside the exchanger to facilitate the required heat flow according to the second law of thermodynamics. In addition, this temperature difference minimizes locally at a certain point inside the exchanger, which is known as the pinch point. In subcritical ORCs with dry and isentropic organic fluids (without superheating), the pinch point in the evaporator occurs on the saturated liquid point 3′, and the pinch point on the condenser occurs at the saturated vapor point 6. The temperature difference ΔT_{pp} at such a pinch point must be optimally designed since it influences both the efficiency and the cost of the heat exchanger. A pinch point temperature difference near zero increases the second law efficiency of the heat exchanger since it tends to operate more reversibly but increases the size and the cost of the exchanger. On the other hand, as the pinch point temperature difference increases, it lowers the efficiency of the heat transfer process. A pinch point temperature difference equal to $\Delta T_{pp} = 10$ °C is normally considered as the optimum value for evaporators and condensers, and in the present study, this value will be considered valid in all cases. Accordingly, the following parameters are defined [59–61]:

$$T_e^* = T_3{}' + \Delta T_{pp} \tag{6}$$

and

$$T_c^* = T_6 - \Delta T_{pp} \tag{7}$$

where $T_3{}'$ is the temperature of the evaporator, and T_6 is the temperature of the condenser. Then, the mass flow rate of the working fluid is given as

$$\dot{m}_f = \frac{\dot{m}_o c_o (T_{o,1} - T_e^*)}{h_4 - h_{3'}} = \frac{\dot{m}_w c_w (T_c^* - T_{w,1})}{h_6 - h_1} \tag{8}$$

This leads to the equation:

$$\frac{T_6 - \Delta T_{pp} - T_{w,1}}{T_{o,1} - T_{3'} - \Delta T_{pp}} = \left(\frac{\dot{m}_w c_w}{\dot{m}_o c_o}\right)\left(\frac{h_6 - h_1}{h_4 - h_{3'}}\right) \tag{9}$$

which may be used for the calculation of the optimum temperature of condensation T_6 assuming an evaporation temperature $T_3{}'$. At the same time, the unknown condensation variables T_6, h_6, and h_1 are calculated through an appropriate iterative procedure.

The overall thermal input to the biomass boiler is:

$$\dot{Q}_{in} = \dot{m}_f(h_4 - h_3) \tag{10}$$

and the heat transferred to the working fluid in the regenerator is given by:

$$\dot{Q}_{regen} = \dot{m}_f(h_3 - h_2) \tag{11}$$

where $\dot{m}_f$ is the mass flow rate of the working fluid. The turbine power output is given by:

$$\dot{W}_T = \dot{m}_f(h_4 - h_5) \tag{12}$$

Finally, the expanded fluid returns to the initial state 1 by passing through the condenser. The heat delivered to the cooling water is calculated as:

$$\dot{Q}_{heat} = \varepsilon_C \dot{m}_f(h_6 - h_1) = \dot{m}_w c_{\mathrm{w}}(T_{w,2} - T_{w,1}) \tag{13}$$

where $\varepsilon_C = 0.8$ is the efficiency of the condenser; $\dot{m}_w$ is the mass flow rate of the cooling water; $h_{w,1}$ is the specific enthalpy of cooling water at temperature $T_{\mathrm{w},1}$= 30 °C, and c_{w} is the specific heat of water. The same equation allows the estimation of the water temperature $T_{w,2}$ at the outlet of the condenser, while the temperature $T_{\mathrm{o},2}$ of oil at the outlet of the evaporator is calculated as:

$$T_{\mathrm{o},2} = T_{\mathrm{o},1} - \frac{\dot{Q}_{in}}{\dot{m}_{\mathrm{o}} c_{\mathrm{o}}} \tag{14}$$

The pump power consumption is calculated as:

$$\dot{W}_p = \dot{m}_f w_{pa} \tag{15}$$

and the mechanical power is calculated as:

$$\dot{W}_{mech} = \dot{W}_T - \dot{W}_p \tag{16}$$

The mechanical efficiency of the plant is:

$$\eta_{mech} = \frac{\dot{W}_{mech}}{\dot{Q}_{in}} \tag{17}$$

and the thermal efficiency for water heating is:

$$\eta_{th} = \frac{\dot{Q}_{heat}}{\dot{Q}_{in}} \tag{18}$$

Finally, the cogeneration efficiency in this study is defined as:

$$\eta_{\mathrm{CHP}} = \frac{\dot{W}_{mech} + \dot{Q}_{heat}}{\dot{Q}_{in}} = \eta_{mech} + \eta_{th} \tag{19}$$

The exergy analysis of the ORC cycle will also be used assuming that the dead state is at $T_0 = 25$ °C and $p_0 = 101.3$ kPa. In addition, the chemical exergy of the fluid flows will be neglected since chemical reactions are not involved. Accordingly, the total physical exergy for each flow stream i of the working fluid is given as:

$$E_i^{PH} = \dot{m}_{f,i}[h_i - h_0 - T_0(s_i - s_0)] \tag{20}$$

and for a stream of liquid j, the associated total physical exergy is:

$$E_j^{PH} = \dot{m}_j c_j \left[T_j - T_0 - T_0 ln\left(\frac{T_j}{T_0}\right) \right] \quad (21)$$

Then, assuming that all the components (pump, evaporator, expander, regenerator, and condenser) of the plant are adiabatic, the exergy destruction rate in each component k of the ORC cycle will be given as:

$$E_{D,k} = \sum_i E_{i,k,in}^{PH} - \sum_i E_{i,kout}^{PH} + \sum_i \dot{W}_{i,k} \quad (22)$$

where $E_{i,in}^{PH}$ corresponds to a flow i entering the component k; $E_{i,out}^{PH}$ corresponds to a flow i exiting the component k, and $\dot{W}_i$ corresponds to mechanical power entering ($\dot{W}_i > 0$) or exiting ($\dot{W}_i < 0$) the component. The exergy destruction rate in each component must be a positive value; otherwise, the second law of thermodynamics is violated, and ORC operation is impossible. In addition, the lower the exergy destruction rate in a component, the more efficient is its operation.

4. Results and Discussion

4.1. Optimal Condensation Pressure

A pinch point analysis was carried out keeping the pinch point temperature differences of the evaporator and the condenser at the optimal value of $\Delta T_{pp} = 10$ °C. Through the iterative calculation, explained above, the optimal condensation pressure was obtained for every fluid assuming different evaporation pressures and temperatures. The results of these calculations are summarized in Figure 3, which gives the ranges of the calculated optimum condensation pressures for each fluid. As shown, depending on the fluid, the condensation pressure, which ensures the desired ΔT_{pp}, may vary from about 0.017 kPa for D6 to almost 2816 kPa for R1234yf. Inside this large spectrum of condensation pressure, three classes of fluids may be distinguished:

- Low condensation pressure fluids with a condensation pressure below 10 kPa.
- Medium condensation pressure fluids with a condensation pressure between 10 and 1000 kPa.
- High condensation pressure fluids with a condensation pressure above 1000 kPa.

The lower the condensation pressure, the higher the efficiency of the ORC is expected to be. However, extremely low condensation pressures need the consumption of energy and cause air infiltration to the condenser. For these reasons, the optimum range of condensation pressure corresponds to about 10–500 kPa. It is important to notice that the condensation pressures in Figure 2 are those that were found feasible for practical operation in the present study and under its specific assumed operation parameters. Different operation parameters may alter the values of the calculated pressures, but the order of magnitude for each specific fluid mentioned in Figure 2 may be considered as typical. For D5 and R125, the calculated condensation pressure was always higher than their corresponding critical pressure, and, as a result, these fluids are not considered appropriate for the ORC plant examined in the present study.

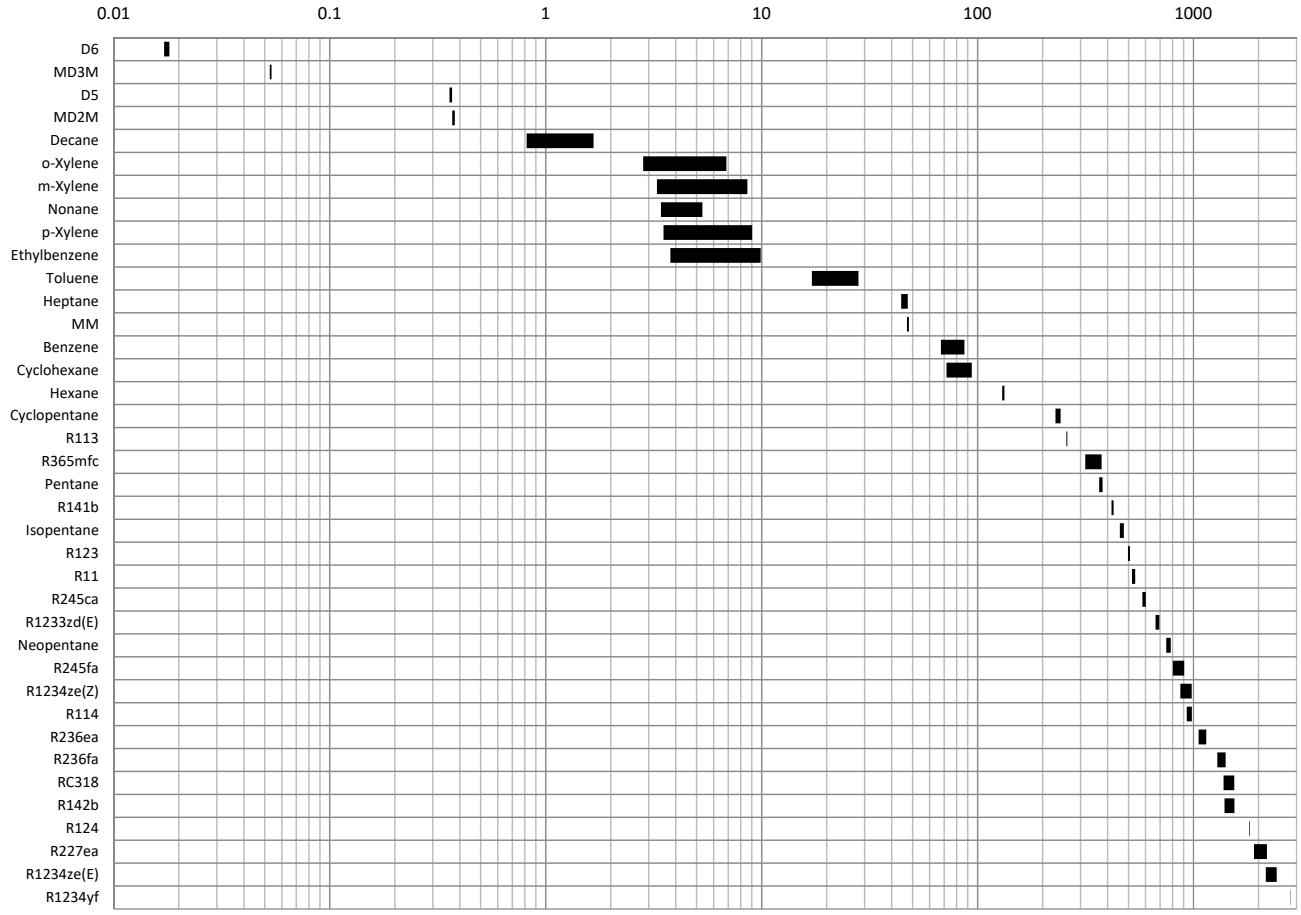

Figure 3. Ranges of calculated condensation pressures (kPa) for each working fluid of the ORC cycle.

4.2. Net Mechanical Power

Waste heat recovery and BB–ORC cogeneration plants intend mainly to convert the capturing heat into useful mechanical power. For the fluids examined in the present study, the effect of the evaporation pressure on the net mechanical power output of the ORC plant is given in Figure 4. Figure 4a illustrates the effect of the evaporation pressure on the mechanical power of the plant when operating with refrigerants and siloxanes. As shown, high power outputs of about 1000–1440 kW are feasible with appropriate fluids, such as MM, MD2M, R113, MD3M (dodecamethylpentasiloxane), R141b, and R365mfc. Of these, the siloxanes MM, MD2M, and MD3M are restricted to operate at low evaporation temperatures due to their low critical temperature but, as shown, their expected power output is in the highest range. A reason behind this behavior is obviously the very low condensation pressure of these fluids as is shown in Figure 3. R113, R141b, and R365mfc, on the contrary, operate at more practical condensation pressures and may provide high power outputs operating at increased evaporation pressures. Figure 4b provides a similar analysis for the hydrocarbon fluids, which are found capable of higher power outputs. Here, power outputs in the range of 1000 to 1950 kW are feasible by a wide variety of fluids, such as nonane, toluene, heptane, cyclohexane, benzene, ethylbenzene, o-xylene, p-xylene, m-xylene, cyclopentane, and hexane. In terms of their condensation pressure, toluene, heptane, benzene, cyclohexane, and cyclopentane seem to be more practical.

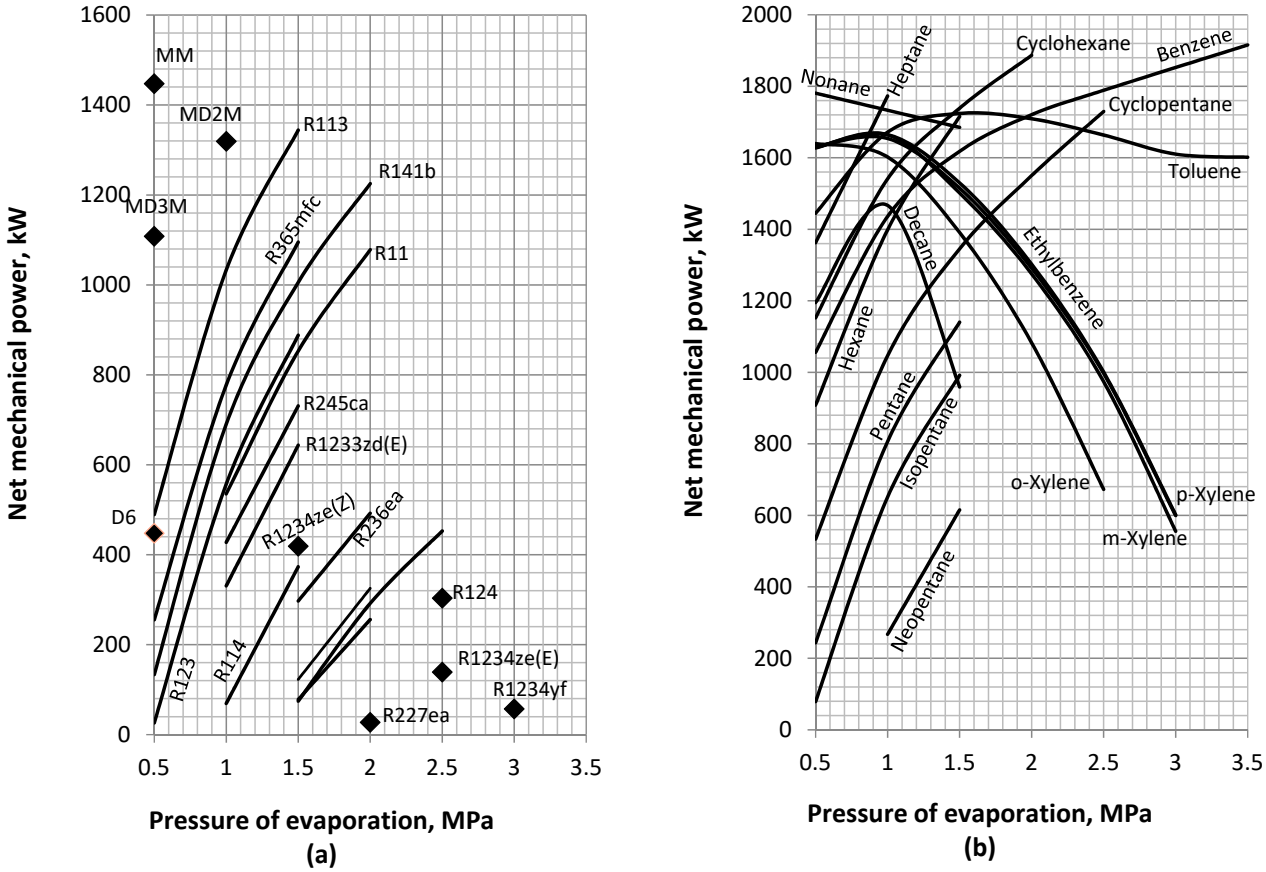

Figure 4. Net mechanical power output of the ORC cycle with refrigerants and siloxanes (**a**) and hydrocarbon (**b**) organic fluids.

4.3. Mechanical and Thermal Efficiency

Figure 5 illustrates the effect of the pressure of the evaporator on the mechanical efficiency of the ORC plant when operating with refrigerants and siloxanes. The situation without internal regeneration is analyzed in Figure 5a, and, as shown, mechanical efficiency attains at best approximately 15%. Again, low condensation pressure siloxanes (D6, MD2M, and MD3M), R141b, R11, and R113 are the most promising options. The effect of the internal regeneration on the mechanical efficiency may be comparatively illustrated in Figure 5b. As observed, in the regenerative cycle, the siloxanes may provide a mechanical efficiency of up to 28%. The effect of the regeneration is more profound in the fluids operating between a high evaporation–condensation pressure difference and also when the mechanical power output becomes significant, usually at higher evaporation pressures. Therefore, the improvement caused by the regeneration is negligible for the fluids in the lower part of the diagram and becomes practical for the fluids that are already efficient in the nonregenerative cycle. Again, the lower condensation pressure seems to be important for an efficient operation, but fluids, such as R113 and R141b, can operate at higher condensation pressures avoiding the problems of energy consumption and air infiltration.

A similar analysis for the cases of hydrocarbons is provided in Figure 6a,b. Without heat, regenerative mechanical efficiencies up to about 26% are possible by low condensation pressure hydrocarbons, such as the xylene isomers, ethylbenzene and decane. Toluene and benzene are also promising, giving mechanical efficiencies above 20% at higher evaporation pressures. In the regenerative ORC cycle, the mechanical efficiencies of all these hydrocarbons are significantly improved. Efficiencies up to 32.5% are now feasible, and toluene is found to exceed 25% at evaporation pressures above 1.5 MPa. As shown previously in Figure 4b, at this pressure range, toluene constantly has a mechanical power output above

1600 kW. Similarly, benzene has a mechanical efficiency higher than 20% and a power capacity higher than 1600 kW at evaporation pressures above 1.5 MPa.

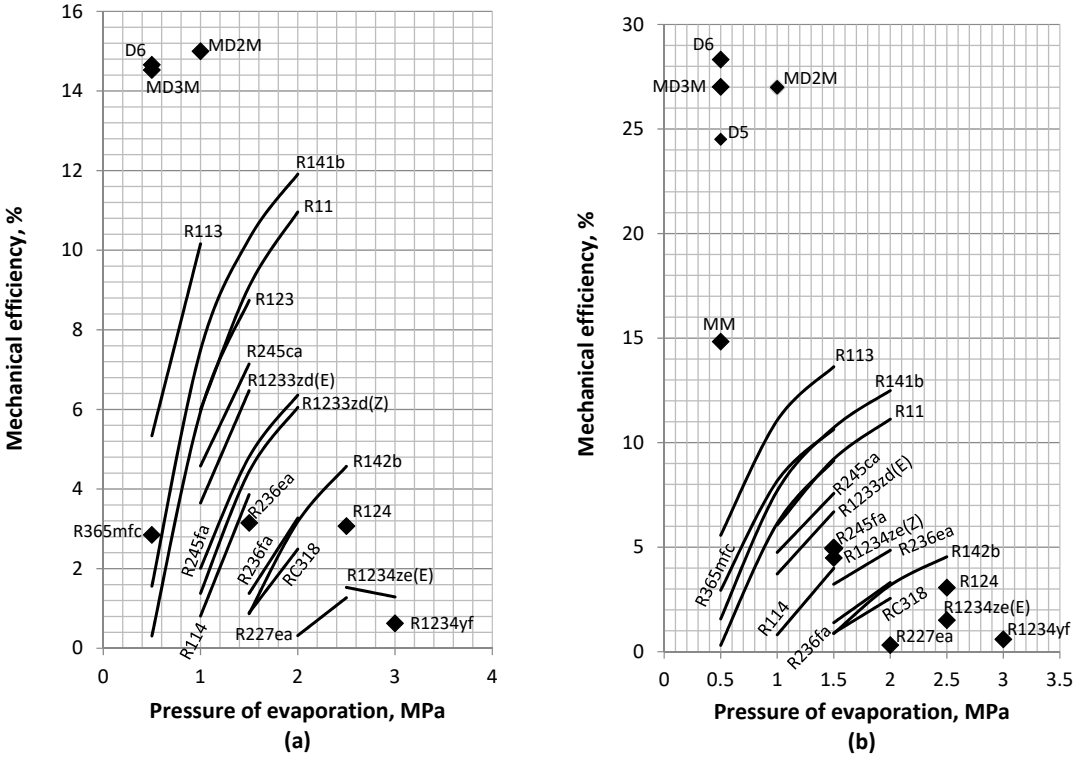

Figure 5. Effect of the evaporation pressure on the mechanical efficiency of the ORC cycle using refrigerants and siloxanes without regeneration (**a**) and with regeneration (**b**).

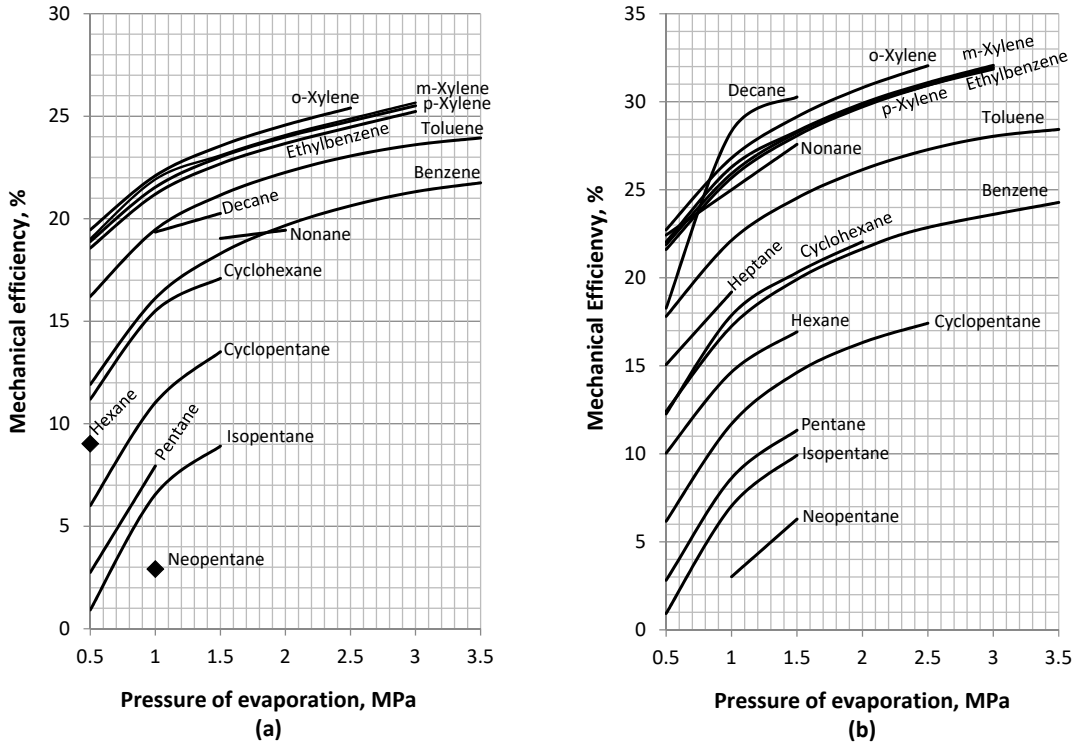

Figure 6. Effect of the evaporation pressure on the mechanical efficiency of the ORC cycle using hydrocarbons without regeneration (**a**) and with regeneration (**b**).

Figure 7 illustrates the thermal efficiency of the regenerative ORC cycle in all the examined fluid cases. As shown, the fluids that were observed to provide the highest mechanical efficiency now provide the lowest thermal efficiency. This is no surprise since heat and work are the two competing outputs of the ORC. Figure 7 corresponds to the ORC using internal regeneration, which maximizes the mechanical efficiency. Refrigerants are shown to favor the production of heat over work, while hydrocarbons and siloxanes seem to favor the production of work over heat. In any case, the results presented in the present study summarize the behavior of a large and representative group of pure organic fluids, which can match the specific needs of an ORC cycle designer or operator. The heat rejected by the ORC plant may be useful for certain purposes, such as space heating, process heating, district heating, etc.

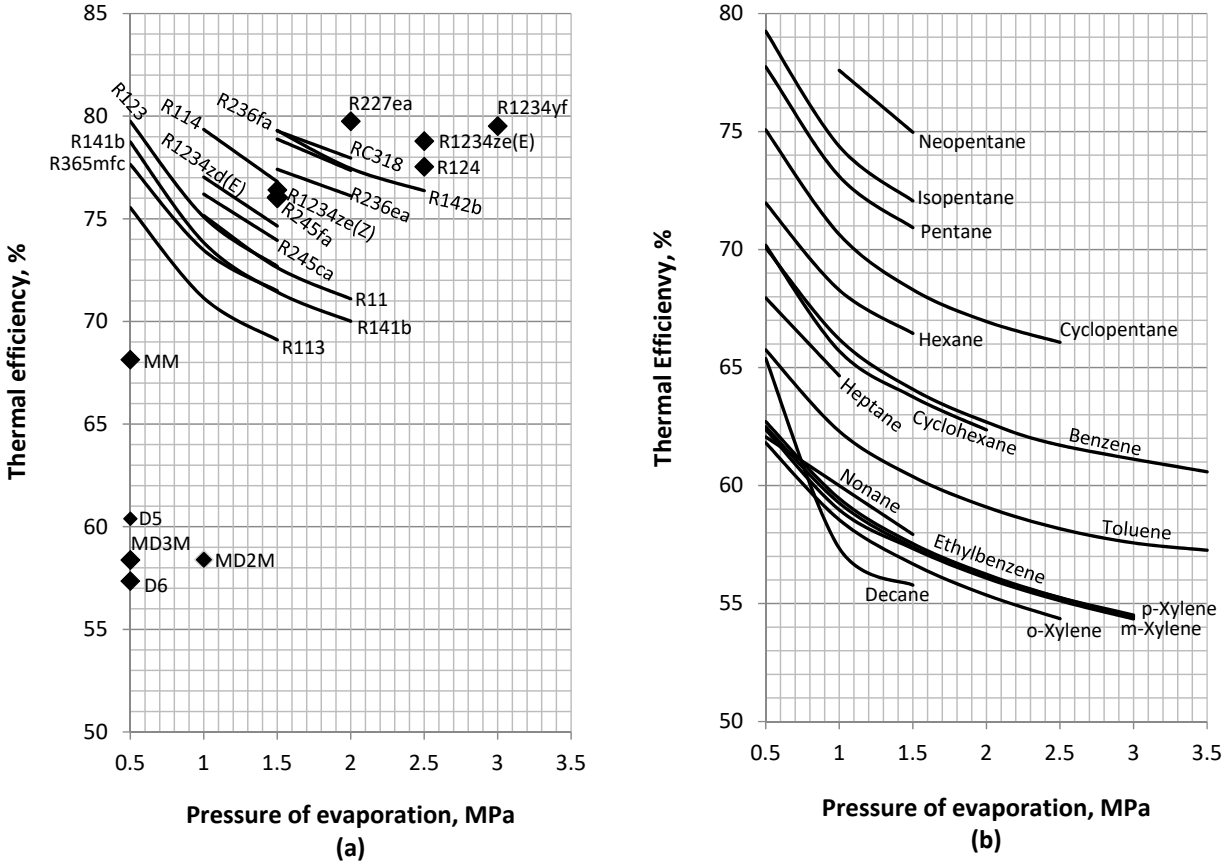

Figure 7. Effect of the evaporation pressure on the thermal efficiency of the ORC cycle using refrigerants and siloxanes (**a**) and hydrocarbon organic fluids (**b**).

4.4. Exergy Analysis

An exergy analysis was employed in the present study to validate the operational feasibility of each examined ORC operation scenario on the basis of the second law of thermodynamics. Through every ORC calculation, the exergy destruction rate inside each ORC component was calculated and checked to be positive. This provided a means to exclude the ORC operation scenarios, which are not thermodynamically feasible, and served as a safe measure for the modeling calculations. Figure 8 illustrates a typical allocation of the exergy destruction rate inside the components of the ORC plant for the case of cyclopentane. In Figure 8a, the case of the regenerative cycle is examined, and, as shown, the operation of the plant is possible with evaporation pressures up to 3.5 MPa. Given that the critical pressure of cyclopentane is 4.57 MPa, one could expect the possibility for operation at pressures higher than 3.5 MPa, but the exergy destruction rate of the evaporator becomes negative at these conditions. This is observed by the reducing trend of the exergy destruction rate of the evaporator in Figure 8a. Similarly, Figure 8b illustrates

the corresponding operation of the nonregenerative cycle and shows that the positive exergy balance is now possible only up to 1.5 MPa. This observation highlights another advantage of the internal heat regeneration that facilitates the operation of the plant at higher evaporation pressures and at higher mechanical efficiencies.

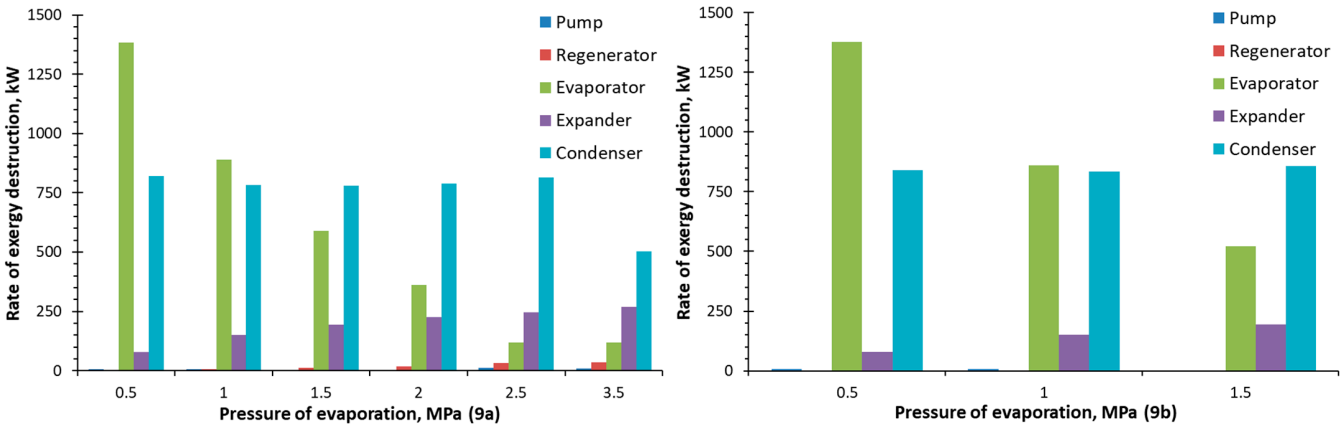

(**a**) (**b**)

Figure 8. Rate of exergy destruction in the ORC cycle equipment using cyclopentane: (**a**) with regeneration, and (**b**) without regeneration.

Figure 8 shows that the main exergy destruction in the plant takes place in the evaporator and the condenser. The exergy destruction inside the expander is much lower but increases as the power output of the turbine increases with pressure. For cyclopentane, the exergy destruction of the pump and the regenerator is almost zero, meaning that their operation is almost reversible. Another example of exergy destruction allocation is given in Figure 9 for the case of o-xylene. In this case, the ORC cycle operation is feasible at the same conditions on both the regenerative and the nonregenerative cycles. In addition, the allocation of the exergy destruction is quite similar in these two cases with the exception, of course, that the exergy destruction of the regenerator in the latter case is zero by definition.

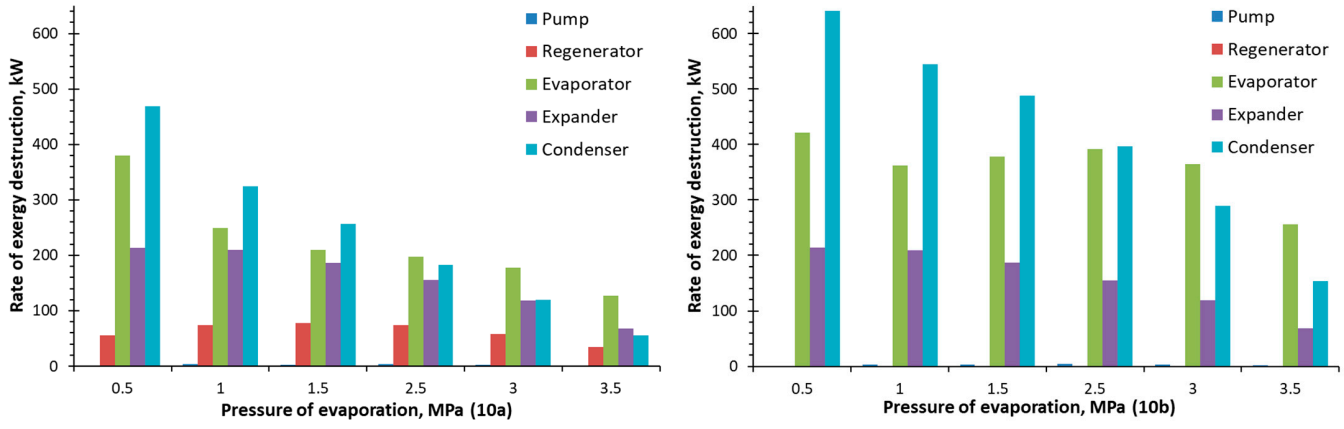

(**a**) (**b**)

Figure 9. Rate of exergy destruction in the ORC cycle equipment using o-xylene: (**a**) with regeneration, and (**b**) without regeneration.

4.5. Selection of the Working Fluid

The analysis presented so far has shown the working fluids with the most favorable thermodynamic performances in terms of mechanical power output, mechanical efficiency, and thermal efficiency. For the specific heat and power cogeneration BB–ORC plant, other important selection parameters are also the temperature $T_{w,2}$ of the hot water produced

in the condenser and the mass flow rate $\dot{m}_f$ of the working fluid. The temperature of the produced warm water is a decisive parameter for the heating purposes of the CHP plant since, for example, some applications, such as residential and domestic heating, require water with a sufficiently high heating capacity. On the other hand, the higher the required mass flow rate of the fluid, the larger the pump and the turbine (expander) devices of the plant have to be, thereby increasing its capital cost.

Table 4 presents a comparative compilation of the calculated results for the examined refrigerants. As mentioned previously, refrigerants provide higher thermal efficiencies than siloxanes and hydrocarbons and are, therefore, more suited for CHP plants aiming at the maximization of the heating capacity and the hot water temperature. Table 4 shows that for all the examined cases, refrigerants are capable to provide hot water with a temperature above 60 °C. It is important to note, however, that in most cases this is achieved at a very low mechanical efficiency, and thus caution is required. Setting a minimum desired mechanical efficiency of about 12%, only R113 and R141b may be considered as appropriate refrigerants at the evaporation pressures of 1.5 and 2 MPa, respectively. A similar analysis is presented also for the hydrocarbons in Table 5. Some of these fluids have been found to optimize the mechanical power, while others were found more appropriate for heating purposes. When high mechanical power and efficiency are desired, a short list of appropriate hydrocarbons is formulated, including cyclopentane, hexane, cyclohexane, heptane, benzene, and toluene. These fluids provide mechanical efficiencies in the range of 14–26% and power outputs above 1300–1880 kW at moderate evaporation pressures between 1 and 2 MPa. In these conditions, the highest power output is 1886.55 kW for cyclohexane at 2 MPa, and the highest mechanical efficiency is 26.14% for toluene at 2 MPa. In addition, ethylbenzene, the xylene m-, o-, and p- isomers; and nonane demonstrate comparable or even higher mechanical performance at lower evaporation pressures between 0.5 and 1.0 MPa. With these fluid options, power outputs of 1620–1650 kW and mechanical efficiencies of 21–26% are attainable at the lower evaporation pressure range but also with condensation pressures below 10 kPa.

All the selected hydrocarbons discussed in the previous paragraph are suitable for high mechanical performance, but when adequate mechanical efficiency and maximum temperature hot water production are needed in combination, cyclopentane and hexane are the most promising. Cyclopentane provides about 1550 kW, 16.32% mechanical efficiency, and hot water temperatures above 60 °C at the evaporation pressure of 2 MPa, while hexane provides more than 1400 kW, more than 14.65% mechanical efficiency, and water temperatures above 60 °C at 1–1.5 MPa. Excluding cyclopentane and hexane, all other hydrocarbons cannot provide in combination sufficient mechanical power and hot water above 60 °C. It is important to note that the demarcation temperature of 60 °C is mentioned here due to the results obtained assuming the ORC plant with the specific operation conditions and with the cold feed water temperature set at 30 °C. In practice, the designer may need hot water of higher temperatures (i.e., 80–90 °C), and this may be achieved by using warmer feed water as it is the case, for example, with the Turboden ORC 10 CHP plant discussed in Table 1. The change of the feed water temperature is not expected to change the relative classification of the examined fluids in terms of mechanical and thermal performance.

Finally, Table 6 presents the calculated results for the examined siloxanes. For D5, D6, MD2M, and MD3M, high mechanical efficiencies (between 24 and 28 %) are attained but at extremely low condensation temperatures and with low temperature water production. The only exception among the examined siloxanes is MM, which has a high condensation pressure of about 47 kPa and gives a sufficiently high mechanical efficiency of about 15 % and water temperatures above 60 °C at the evaporation pressure of 0.5 MPa.

Table 4. Comparative presentation of the results for the refrigerants assumed in the present study.

Working Fluid	P_{vap} (MPa)	$\dot{m}_f$ (kg/s)	$\dot{W}_{mech}$ (kW)	With Regeneration					Without Regeneration				
				η_{mech} (%)	η_{th} (%)	η_{CHP} (%)	$T_{w,2}$ (°C)	$T_{o,2}$ (°C)	η_{mech} (%)	η_{th} (%)	η_{CHP} (%)	$T_{w,2}$ (°C)	$T_{o,2}$ (°C)
R11	1	52.48	535.47	6.06	75.15	81.21	61.7	75.4	6	75.2	81.2	62.1	72.7
	1.5	53.03	853.14	9.22	72.62	81.84	62.1	62.7	9.09	72.73	81.82	62.6	58.5
	2	54.62	1078.19	11.12	71.1	82.22	62.9	48.8	10.96	71.23	82.19	63.5	44.5
R113	0.5	61.32	489.33	5.57	75.54	81.11	61.7	77.4	5.34	75.73	81.07	63.2	65.2
	1	60.52	1033.02	11.07	71.14	82.21	61.7	60.2	10.16	71.88	82.03	64.9	34
	1.5	61.74	1344.24	13.63	69.1	82.73	62.6	43.6	-	-	-	-	-
R114	1	82.88	69.34	0.81	79.35	80.16	62.3	85.5	0.81	79.35	80.16	62.5	84
	1.5	88.87	373.25	3.99	76.81	80.8	64.3	59.3	3.86	76.91	80.77	65.6	49.4
R123	0.5	57.52	26.08	0.31	79.75	80.06	62	89.2	0.31	79.75	80.06	62	89.1
	1	58.12	556.97	6.14	75.09	81.23	62.6	68.1	5.94	75.24	81.19	63.7	59
	1.5	60.21	888.19	9.14	72.69	81.83	63.7	48.3	8.74	73.01	81.75	65.4	34.3
R124	2.5	98.24	303.83	-	-	-	-	-	3.07	77.54	80.61	66.7	42.6
R141b	0.5	42.19	133.55	1.57	78.74	80.31	61.9	86.6	1.56	78.75	80.31	62.1	84.9
	1	41.54	690.42	7.7	73.84	81.54	61.6	71.5	7.49	74.01	81.5	62.6	63.7
	1.5	41.84	1005.78	10.72	71.43	82.14	62	58.5	10.29	71.76	82.06	63.5	46.5
	2	42.98	1225.11	12.49	70.01	82.5	62.8	45.2	11.91	70.47	82.38	64.6	30.6
R142b	1.5	54.35	74.56	0.87	79.3	80.17	62.3	85	0.87	79.3	80.17	62.3	85
	2	57.99	291.98	3.18	77.45	80.64	63.9	65.2	3.18	77.45	80.64	64	65
	2.5	63.52	452.81	4.54	76.37	80.91	66.4	40.4	4.57	76.35	80.91	66.2	42.2
R227ea	2	130.31	27.49	0.32	79.75	80.06	63	80.6	0.32	79.75	80.06	63.1	80
	2.5	174.33	124.51	-	-	-	-	-	1.27	78.99	80.25	67	45.1
R236ea	1.5	74.51	297.26	3.23	77.41	80.65	64	64.4	3.15	77.48	80.63	65	56.6
	2	82.58	492.28	4.85	76.12	80.97	66.9	34.9	-	-	-	-	-
R236fa	1.5	82.92	122.89	1.39	78.88	80.28	63.2	76.4	1.38	78.89	80.28	63.5	73.7
	2	94.19	325.23	3.31	77.36	80.66	66.4	44.4	3.27	77.39	80.65	66.8	40.8
R245ca	1	50.15	427.55	4.75	76.2	80.95	62.8	70.3	4.58	76.34	80.92	64	60.1
	1.5	52.15	730.93	7.57	73.95	81.51	64.1	50	7.14	74.29	81.43	66.3	32
	1	50.15	427.55	4.58	76.34	80.92	64	60.1	-	-	-	-	-
	1.5	52.15	730.93	7.14	74.29	81.43	66.3	32	-	-	-	-	-
R245fa	1	55.41	177.11	-	-	-	-	-	2.01	78.39	80.4	63	76.6
	1.5	58.76	467.91	4.95	76.04	80.99	64.3	56.5	4.81	76.16	80.96	65.4	47.6
R365mfc	0.5	50.12	255.39	2.94	77.65	80.59	62.2	80.2	2.85	77.72	80.57	63.3	71.7
	1	51.07	777.39	8.17	73.47	81.63	63.4	54.3	-	-	-	-	-
	1.5	53.64	1095.21	10.64	71.49	82.13	65.2	30.3	-	-	-	-	-
RC318	1.5	121.32	78.1	0.9	79.28	80.18	63	79.4	0.89	79.29	80.18	63.4	76.2
	2	146.08	255.89	2.55	77.96	80.51	67.3	38.7	2.49	78.01	80.5	68.3	30.7
R1233zd(E)	1	54.16	330.85	3.72	77.03	80.74	62.7	73.6	3.65	77.08	80.73	63.4	68.4
	1.5	56.95	643.6	6.69	74.65	81.34	64.3	51	6.47	74.82	81.29	65.6	41.1
R1234yf	3	145.82	57.35	0.6	79.52	80.12	66.1	55.2	0.63	79.5	80.13	64.72	66.4
R1234ze(E)	2.5	86.86	139.41	1.51	78.79	80.3	64.7	63.8	1.53	78.77	80.31	64.2	67.4
	3	108.13	128.44	-	-	-	-	-	1.29	78.97	80.26	67.5	40.9
R1234ze(Z)	-	-	-	-	-	-	-	-	1.38	78.89	80.28	62.5	82.5
	1.5	54.64	419.06	4.49	76.41	80.9	64.1	60.1	4.44	76.45	80.89	64.5	56.9
	-	-	-	-	-	-	-	-	6.05	75.16	81.21	66.9	30.9

Table 5. Comparative presentation of the results for the hydrocarbons assumed in the present study.

Working Fluid	P_{vap} (MPa)	$\dot{m}_f$ (kg/s)	$\dot{W}_{mech}$ (kW)	With Regeneration					Without Regeneration				
				η_{mech} (%)	η_{th} (%)	η_{CHP} (%)	$T_{w,2}$ (°C)	$T_{o,2}$ (°C)	η_{mech} (%)	η_{th} (%)	η_{CHP} (%)	$T_{w,2}$ (°C)	$T_{o,2}$ (°C)
Pentane	0.5	26.14	243.43	2.82	77.74	80.56	62	82.3	2.75	77.8	80.55	62.9	75.2
	1	26.21	806.47	8.62	73.1	81.72	62.7	59.6	7.94	73.65	81.59	65.8	34.3
	1.5	27.18	1140.32	11.34	70.93	82.27	64.1	37.6	-	-	-	-	-
IsoPentane	0.5	28.15	78.9	0.93	79.25	80.19	62	87.2	0.92	79.26	80.18	62.3	85
	1	28.37	651.11	7.04	74.37	81.41	62.8	62.8	6.55	74.76	81.31	65.5	41.2
	1.5	29.54	991.67	9.92	72.06	81.98	64.4	39.5	-	-	-	-	-
Cyclopentane	0.5	22.03	533.51	6.17	75.07	81.23	61	81.3	6.01	75.19	81.2	61.9	74.2
	1	21.14	1046.23	11.7	70.64	82.34	60.2	72.2	11.03	71.18	82.21	62.3	55.3
	1.5	20.84	1345.52	14.62	68.3	82.92	60	64.2	13.51	69.19	82.7	62.9	40.6
	2	20.98	1550.21	16.32	66.95	83.26	60.4	54.9	-	-	-	-	-
	2.5	21.66	1729.53	17.42	66.07	83.48	61.3	41.5	-	-	-	-	-

Table 5. *Cont.*

Working Fluid	P_{vap} (MPa)	$\dot{m}_f$ (kg/s)	$\dot{W}_{mech}$ (kW)	With Regeneration					Without Regeneration				
				η_{mech} (%)	η_{th} (%)	η_{CHP} (%)	$T_{w,2}$ (°C)	$T_{o,2}$ (°C)	η_{mech} (%)	η_{th} (%)	η_{CHP} (%)	$T_{w,2}$ (°C)	$T_{o,2}$ (°C)
NeoPentane	1	34.23	267.2	3.02	77.59	80.6	62.8	74.8	2.91	77.67	80.58	64.1	64.7
	1.5	36.43	615.1	6.29	74.97	81.26	65	46.4	—	—	—	—	—
Hexane	0.5	24.03	908.19	10.04	71.97	82.01	61.1	69	9.02	72.78	81.8	65	37.2
	1	23.47	1398.71	14.65	68.28	82.93	61.2	53.5	-	-	-	-	-
	1.5	23.94	1715.48	16.93	66.45	83.39	62.2	35.4	-	-	-	-	-
Cyclohexane	0.5	22.39	1152.51	12.27	70.18	82.45	61.5	58.2	11.2	71.04	82.24	64.9	30.3
	1	18.65	1541.17	17.87	65.7	83.57	57.1	82.1	15.5	67.6	83.1	62.1	41.2
	1.5	17.69	1738.7	20.3	63.76	84.06	56.1	84	17.09	66.33	83.42	62.2	34
	2	17.09	1886.55	22.05	62.36	84.41	55.5	84.2	-	-	-	-	-
Heptane	0.5	21.7	1362.57	15.07	67.95	83.01	59.4	69.1	-	-	-	-	-
	1	20.45	1772.89	19.19	64.65	83.84	58.5	63	-	-	-	-	-
Nonane	0.5	16.17	1780.78	22.43	62.06	84.49	53.5	103.4	-	-	-	-	-
	1.5	10.87	1685.07	27.58	57.93	85.52	46.9	160.2	19.04	64.77	83.81	57.4	75.1
	2	10.23	1672.53	-	-	-	-	-	19.44	64.45	83.89	56.5	82.7
Decane	0.5	13.32	1195.17	18.28	65.38	83.66	50.4	146.9	-	-	-	-	-
	1	9.03	1466.69	28.33	57.34	85.67	44.2	189.1	19.35	64.52	83.87	53.4	114.5
	1.5	5.22	958.95	30.27	55.78	86.05	38.4	251.6	20.26	63.79	84.05	44.4	203
Benzene	0.5	18.53	1055.77	12.42	70.07	82.48	58.5	85.9	11.92	70.47	82.38	59.8	74.9
	1	16.89	1435.87	17.25	66.2	83.45	56.3	91.4	16.12	67.1	83.22	58.5	73.4
	1.5	15.8	1618.02	19.91	64.08	83.98	54.9	97.5	18.3	65.36	83.66	57.6	75.4
	2	15.01	1720.53	21.64	62.69	84.33	53.8	103	19.67	64.26	83.93	56.8	78.3
	2.5	14.46	1788.82	22.86	61.71	84.57	53.1	107	20.63	63.5	84.13	56.3	80.6
	3.5	14.26	1915.6	24.28	60.58	84.86	52.8	104.9	21.75	62.6	84.35	56.3	76.4
EthylBenzene	0.5	14.93	1628.79	21.61	62.71	84.32	52.6	115.9	18.57	65.15	83.71	57.3	77.5
	1	11.84	1664.73	25.68	59.45	85.14	48.4	148.6	21.2	63.04	84.24	53.6	106.1
	1.5	9.45	1529.72	28.07	57.54	85.61	45	180.7	22.68	61.86	84.54	49.9	140.4
	2	7.33	1302.39	29.71	56.24	85.94	41.7	213.8	23.67	61.06	84.73	46.1	179.1
	2.5	5.25	1000.7	30.94	55.25	86.19	38.5	249.5	24.47	60.43	84.89	41.8	222.9
	3	2.99	601.28	31.95	54.44	86.39	34.9	291.5	25.23	59.81	85.05	36.8	276
Toluene	0.5	16.78	1444.9	17.81	65.75	83.56	55.5	98	16.21	67.03	83.24	58.5	73.2
	1	14.49	1671.51	22.13	62.3	84.43	52.5	115.4	19.47	64.43	83.89	56.4	83.3
	1.5	12.89	1723.94	24.53	60.38	84.91	50.3	131.7	21.15	63.08	84.23	54.5	96.9
	2	11.62	1709.19	26.14	59.09	85.23	48.4	146.9	22.26	62.19	84.45	52.8	111.5
	2.5	10.59	1663.63	27.28	58.17	85.46	46.9	160.6	23.06	61.55	84.61	51.2	125.9
	3	9.83	1610.27	28.04	57.57	85.61	45.8	171.6	23.61	61.11	84.72	49.9	138.1
	3.5	9.58	1601.61	28.43	57.26	85.69	45.4	175	23.94	60.84	84.79	49.4	142.2
m-Xylene	0.5	14.36	1627.59	22.04	62.37	84.41	52	120.6	19.02	64.78	83.8	56.5	84.2
	1	11.35	1664.42	26.29	58.97	85.26	47.8	153.3	21.92	62.47	84.38	52.6	114.1
	1.5	9.07	1501.43	28.33	57.33	85.67	44.5	185.4	23.09	61.53	84.62	49.1	148
	2	7.05	1275.27	29.91	56.08	85.98	41.4	217.5	24.08	60.74	84.82	45.3	185.5
	2.5	5.04	973.81	31.09	55.12	86.22	38.2	252.7	24.88	60.1	84.98	41.2	228.4
	3	2.73	555.44	32.07	54.35	86.41	34.5	296.2	25.66	59.47	85.13	36.1	282.7
o-Xylene	0.5	13.59	1639.73	22.73	61.81	84.55	51.3	125.9	19.46	64.44	83.89	55.9	88.2
	1	10.38	1602.08	26.81	58.55	85.36	46.7	164.4	22.1	62.32	84.42	51.6	124.8
	1.5	7.87	1390.83	29.15	56.68	85.83	42.9	201.8	23.55	61.16	84.71	47.2	166.5
	2	5.59	1082.58	30.8	55.36	86.16	39.3	240.8	24.57	60.34	84.91	42.7	213.1
	2.5	3.24	672.57	32.05	54.36	86.41	35.4	284.8	25.4	59.68	85.08	37.5	267.7
p-Xylene	0.5	14.64	1630.87	21.89	62.49	84.38	52.2	118.6	18.89	64.89	83.78	56.7	81.9
	1	11.59	1654.09	25.92	59.26	85.18	48	151.8	21.54	62.77	84.31	53	111.5
	1.5	9.27	1514.85	28.25	57.4	85.65	44.7	183.4	23.01	61.59	84.6	49.4	145.5
	2	7.23	1291.12	29.81	56.15	85.96	41.6	215.4	23.99	60.81	84.8	45.6	182.8
	2.5	5.24	996.83	30.94	55.25	86.19	38.5	249.9	24.76	60.2	84.95	41.5	224.9
	3	3	599.43	31.86	54.51	86.37	34.9	291.5	25.51	59.59	85.1	36.6	277

Table 6. Comparative presentation of the results for the siloxanes assumed in the present study.

Working Fluid	P_{vap} (MPa)	$\dot{m}_f$ (kg/s)	$\dot{W}_{mech}$ (kW)	With Regeneration					Without Regeneration				
				η_{mech} (%)	η_{th} (%)	η_{CHP} (%)	$T_{w,2}$ (°C)	$T_{o,2}$ (°C)	η_{mech} (%)	η_{th} (%)	η_{CHP} (%)	$T_{w,2}$ (°C)	$T_{o,2}$ (°C)
D5	0.5	20.22	1429.29	24.51	60.39	84.9	46.8	168.8	-	-	-	-	-
D6	0.5	5	447.79	28.32	57.35	85.66	34.3	300.8	14.66	68.27	82.93	39.9	255.1
MD2M	1	14.41	1319.54	27	58.4	85.4	43.6	198.2	15	68	83	58.6	76.8
MD3M	0.5	12.49	1108.29	27.02	58.38	85.4	41.4	222.6	14.53	68.38	82.91	54.9	113
MM	0.5	36.77	1447.47	14.83	68.13	82.97	61.8	46.9	-	-	-	-	-

A final selection of the working fluids must take additionally into account some important environmental and safety criteria, as follows:

- Dry and isentropic hydrocarbons have shown high thermodynamic performance in the ORC equipped with internal regeneration and also have minimal ozone and global warming impact. They are also nontoxic, but due to their high flammability, they need special safety measures for handling and operation. Despite this drawback, hydrocarbons are generally considered rational fluid options in organic Rankine cycles.
- Chlorofluorocarbons (CFCs) have been banned, and therefore fluids such as R11, R113 and R114 that have shown high thermodynamic performance, must be excluded from the final selection list of working fluids.
- The Kigali Amendment of the Montreal Protocol on Substances that Deplete the Ozone Layer has called for the phase-out of hydrochlorofluorocarbons (HCFCs) after 2016. Therefore, various countries have already planned the gradual substitution of HCFCs in the near future. As a result, refrigerants, such as R123, R124, R141b, and R142b must be excluded from the final selection.
- Fluids with an ODP value above 1 and a GWP value above 2500 will be excluded from the final selection.

Combining the results of the previous discussions with these criteria and constraints, one can arrive at the following final set of guidelines:

- Refrigerants are not appropriate options for BB–ORC plants since they demonstrate extremely low mechanical efficiencies or they are banned for environmental issues.
- Siloxanes demonstrate extremely high mechanical efficiencies at low evaporation pressures but very low thermal efficiencies and hot water temperatures. Moreover, they operate at extremely low and often impractical condensing pressures.
- Hydrocarbons are found to lie in the optimum middle range of the fluid spectrum, between the siloxanes that maximize the production of mechanical power and the refrigerants that maximize the production of heat. Most of them also operate at the practical medium range of condensing pressures between 10 and 1000 kPa.
- When the maximization of mechanical power output is of paramount importance, specific hydrocarbons, such as ethylbenzene, the xylene m-, o-, and p- isomers; and nonane are appropriate options if condensation pressures below 10 kPa can be attained. These fluids can operate at relative low evaporation pressures (0.5–1 MPa) and may be further classified depending on their mass flow rate during operation on the order o-xylene (10.38–13.59 kg/s), m-xylene (11.35–14.36 kg/s), p-xylene (11.59–14.64 kg/s), ethylbenzene (11.84–14.93 kg/s), and nonane (10.87–16.17 kg/s). At higher condensation pressures, cyclopentane, hexane, cyclohexane, heptane, benzene, and toluene are found to be the most appropriate fluids. These can be used at moderate evaporation pressures of 1–2 MPa. In this group, toluene has the lowest mass flow rate (9.58–16.78 kg/s) followed by benzene (14.26–18.53 kg/s), cyclohexane (17.69–22.03 kg/s), heptane (20.45–21.7 kg/s), cyclopentane (20.45–21.7 kg/s), and, finally, hexane (23.47–24.03 kg/s).
- For efficient CHP applications with adequately high mechanical performance and high temperature water production, cyclopentane, hexane, and MM are the most appropriate fluids. According to their mass flow rates, these are classified in the order cyclopentane (20.45–21.7 kg/s), hexane (23.47–24.03 kg/s), and MM (36.77 kg/s).

5. Conclusions

A comparative study was presented for forty-two (42) dry and isentropic refrigerants, hydrocarbons, and siloxanes for subcritical BB–CHP plants and ORC waste heat recovery applications. The cases with and without internal heat regeneration have been examined, and an optimization procedure was applied to fix the pinch point temperatures of the evaporator and the condenser at the optimal value of 10 °C. After the calculation of the appropriate condensation pressure for each working fluid and evaporation pressure, the first and second law analysis was undertaken for each subcritical ORC operation scenario

to provide the relative classification of the working fluids in terms of mechanical power, mechanical efficiency, thermal efficiency, and produced water temperature. Environmental and safety criteria were also taken under consideration. The results of this study provide an original and unique screening of almost all pure working fluids, which are considered appropriate in the literature under the same operation and optimization conditions, and compiles them into a single reference. In addition, they formulate useful fluid selection and system design guidelines, which may be easily followed depending on the optimization objective of the ORC user. For maximum mechanical power and efficiency, ethylbenzene, the xylene m-, o-, and p- isomers; and nonane were found as appropriate fluid options if condensation pressures below 10 kPa can be attained. Since at such low pressures, air infiltration in the condenser and vacuum production costs may be significant problems, other hydrocarbon fluids with comparable performance at higher condensation pressures, such as cyclopentane, hexane, cyclohexane, heptane, benzene, and toluene are considered more practical options. When high-temperature water production is also important, cyclopentane, hexane, and MM (hexamethyldisiloxane) are found as the most appropriate fluids. In general, hydrocarbons are found to lie in the optimum middle range of the fluid spectrum, between siloxanes, which maximize the production of mechanical power, and refrigerants that maximize the production of heat.

Author Contributions: Conceptualization, S.L.D.; methodology, S.L.D.; validation, S.L.D. and A.T.; formal analysis, N.D.C. and M.S.; investigation, S.L.D. and A.T.; writing—original draft preparation, S.L.D.; writing—review and editing, M.S., N.D.C., N.T. and V.K.; supervision, S.L.D.; project administration, S.L.D.; funding acquisition, M.S. and N.T. All authors have read and agreed to the published version of the manuscript.

Funding: This research was funded by the project "Development of New Innovative Low Carbon Footprint Energy Technologies to Enhance Excellence in the Region of Western Macedonia" (MIS 5047197), which is implemented under the Action "Reinforcement of the Research and Innovation Infrastructure", funded by the Operational Programme "Competitiveness, Entrepreneurship and Innovation" (NSRF 2014–2020), and cofinanced by Greece and the European Union (European Regional Development Fund).

Conflicts of Interest: The authors declare no conflict of interest.

Abbreviations

Biomass Boiler–Organic Rankine Cycle	BB–ORC
Chlorofluorocarbons	CFCs
Combined Heat and Power	CHP
Decamethylcyclopentasiloxane	D5
Decamethyltetrasiloxane	MD2M
Dodecamethylcyclohexasiloxane	D6
Dodecamethylpentasiloxane	MD3M
Global Warming Potential	GWP
Hexamethyldisiloxane	MM
Hydrocarbons	HCs
Hydrochlorofluorocarbons	HCFCs
Hydrofluorocarbons	HFCs
Hydrolfluoroolefins	HFOs
Medium Density Fiberboards	MDFs
Octamethyltrisiloxane	MDM
Organic Rankine Cycles	ORCs
Ozone Depletion Potential	ODP
Perfluorocarbons	PFCs

References

1. Zalasiewicz, J.; Waters, C.N.; Summerhayes, C.P.; Wolfe, A.P.; Barnosky, A.D.; Cearreta, A.; Crutzen, P.; Ellis, E.; Fairchild, I.J.; Gałuszka, A.; et al. The Working Group on the Anthropocene: Summary of Evidence and Interim Recommendations. *Anthropocene* **2017**, *19*, 55–60. [CrossRef]
2. Chen, S.; Liu, P.; Li, Z. Low Carbon Transition Pathway of Power Sector with High Penetration of Renewable Energy. *Renew. Sustain. Energy Rev.* **2020**, *130*, 109985. [CrossRef]
3. Genus, A.; Iskandarova, M. Transforming the Energy System? Technology and Organisational Legitimacy and the Institutionalisation of Community Renewable Energy. *Renew. Sustain. Energy Rev.* **2020**, *125*, 109795. [CrossRef]
4. Inayat, A.; Raza, M. District Cooling System via Renewable Energy Sources: A Review. *Renew. Sustain. Energy Rev.* **2019**, *107*, 360–373. [CrossRef]
5. Douvartzides, S.L.; Charisiou, N.D.; Papageridis, K.N.; Goula, M.A. Green Diesel: Biomass Feedstocks, Production Technologies, Catalytic Research, Fuel Properties and Performance in Compression Ignition Internal Combustion Engines. *Energies* **2019**, *12*, 809. [CrossRef]
6. Charisiou, N.D.; Polychronopoulou, K.; Asif, A.; Goula, M.A. The Potential of Glycerol and Phenol towards H2 Production Using Steam Reforming Reaction: A Review. *Surf. Coat. Technol.* **2018**, *352*, 92–111. [CrossRef]
7. Sharma, H.B.; Sarmah, A.K.; Dubey, B. Hydrothermal Carbonization of Renewable Waste Biomass for Solid Biofuel Production: A Discussion on Process Mechanism, the Influence of Process Parameters, Environmental Performance and Fuel Properties of Hydrochar. *Renew. Sustain. Energy Rev.* **2020**, *123*, 109761. [CrossRef]
8. Ong, H.C.; Chen, W.-H.; Singh, Y.; Gan, Y.Y.; Chen, C.-Y.; Show, P.L. A State-of-the-Art Review on Thermochemical Conversion of Biomass for Biofuel Production: A TG-FTIR Approach. *Energy Convers. Manag.* **2020**, *209*, 112634. [CrossRef]
9. IEA Bioenergy. Electricity from Biomass: From Small to Large Scale. In *Summary and Conclusions from the IEA Bioenergy ExCo72 Workshop*; IEA Bioenergy: Göteborg, Sweden, 2015.
10. Oyekale, J.; Petrollese, M.; Heberle, F.; Brüggemann, D.; Cau, G. Exergetic and Integrated Exergoeconomic Assessments of a Hybrid Solar-Biomass Organic Rankine Cycle Cogeneration Plant. *Energy Convers. Manag.* **2020**, *215*, 112905. [CrossRef]
11. Wang, Q.; Wu, W.; He, Z. Thermodynamic Analysis and Optimization of a Novel Organic Rankine Cycle-Based Micro-Scale Cogeneration System Using Biomass Fuel. *Energy Convers. Manag.* **2019**, *198*, 111803. [CrossRef]
12. Modi, A.; Bühler, F.; Andreasen, J.G.; Haglind, F. A Review of Solar Energy Based Heat and Power Generation Systems. *Renew. Sustain. Energy Rev.* **2017**, *67*, 1047–1064. [CrossRef]
13. Rayegan, R.; Tao, Y.X. A Procedure to Select Working Fluids for Solar Organic Rankine Cycles (ORCs). *Renew. Energy* **2011**, *36*, 659–670. [CrossRef]
14. Tchanche, B.F.; Lambrinos, G.; Frangoudakis, A.; Papadakis, G. Low-Grade Heat Conversion into Power Using Organic Rankine Cycles—A Review of Various Applications. *Renew. Sustain. Energy Rev.* **2011**, *15*, 3963–3979. [CrossRef]
15. Tchanche, B.F.; Pétrissans, M.; Papadakis, G. Heat Resources and Organic Rankine Cycle Machines. *Renew. Sustain. Energy Rev.* **2014**, *39*, 1185–1199. [CrossRef]
16. Vélez, F.; Segovia, J.J.; Martín, M.C.; Antolín, G.; Chejne, F.; Quijano, A. A Technical, Economical and Market Review of Organic Rankine Cycles for the Conversion of Low-Grade Heat for Power Generation. *Renew. Sustain. Energy Rev.* **2012**, *16*, 4175–4189. [CrossRef]
17. Tzivanidis, C.; Bellos, E.; Antonopoulos, K.A. Energetic and Financial Investigation of a Stand-Alone Solar-Thermal Organic Rankine Cycle Power Plant. *Energy Convers. Manag.* **2016**, *126*, 421–433. [CrossRef]
18. Bellos, E.; Tzivanidis, C. Parametric Analysis and Optimization of an Organic Rankine Cycle with Nanofluid Based Solar Parabolic Trough Collectors. *Renew. Energy* **2017**, *114*, 1376–1393. [CrossRef]
19. Heberle, F.; Brüggemann, D. Exergy Based Fluid Selection for a Geothermal Organic Rankine Cycle for Combined Heat and Power Generation. *Appl. Therm. Eng.* **2010**, *30*, 1326–1332. [CrossRef]
20. Javanshir, A.; Sarunac, N.; Razzaghpanah, Z. Thermodynamic Analysis of ORC and Its Application for Waste Heat Recovery. *Sustainability* **2017**, *9*, 1974. [CrossRef]
21. Jouhara, H.; Khordehgah, N.; Almahmoud, S.; Delpech, B.; Chauhan, A.; Tassou, S.A. Waste Heat Recovery Technologies and Applications. *Therm. Sci. Eng. Prog.* **2018**, *6*, 268–289. [CrossRef]
22. Xu, B.; Rathod, D.; Yebi, A.; Filipi, Z.; Onori, S.; Hoffman, M. A Comprehensive Review of Organic Rankine Cycle Waste Heat Recovery Systems in Heavy-Duty Diesel Engine Applications. *Renew. Sustain. Energy Rev.* **2019**, *107*, 145–170. [CrossRef]
23. Pantaleo, A.M.; Camporeale, S.; Fortunato, B. Small Scale Biomass CHP: Techno-Economic Performance of Steam vs Gas Turbines with Bottoming ORC. *Energy Procedia* **2015**, *82*, 825–832. [CrossRef]
24. Qiu, G.; Shao, Y.; Li, J.; Liu, H.; Riffat, S.B. Experimental Investigation of a Biomass-Fired ORC-Based Micro-CHP for Domestic Applications. *Fuel* **2012**, *96*, 374–382. [CrossRef]
25. Nur, T.B.; Syahputra, A.W. Integrated Biomass Pyrolysis with Organic Rankine Cycle for Power Generation. In Proceedings of the 10th International Conference Numerical Analysis in Engineering, Banda Aceh, Indonesia, 24–25 August 2017; Volume 308, p. 012030. [CrossRef]

26. Nur, T.B.; Pane, Z.; Amin, M.N. Application of Biomass from Palm Oil Mill for Organic Rankine Cycle to Generate Power in North Sumatera Indonesia. In Proceedings of the 1st Annual Applied Science and Engineering Conference (AASEC), in Conjuction with The International Conference on Sport Science, Health, Bandung, Indonesia, 16–18 November 2016, and Physical Education (ICSSHPE); Volume 180, p. 012035. [CrossRef]
27. Algieri, A.; Morrone, P. Techno-Economic Analysis of Biomass-Fired ORC Systems for Single-Family Combined Heat and Power (CHP) Applications. *Energy Procedia* **2014**, *45*, 1285–1294. [CrossRef]
28. Eyidogan, M.; Canka Kilic, F.; Kaya, D.; Coban, V.; Cagman, S. Investigation of Organic Rankine Cycle (ORC) Technologies in Turkey from the Technical and Economic Point of View. *Renew. Sustain. Energy Rev.* **2016**, *58*, 885–895. [CrossRef]
29. Zhu, Y.; Li, W.; Li, J.; Li, H.; Wang, Y.; Li, S. Thermodynamic Analysis and Economic Assessment of Biomass-Fired Organic Rankine Cycle Combined Heat and Power System Integrated with CO_2 Capture. *Energy Convers. Manag.* **2020**, *204*, 112310. [CrossRef]
30. Imran, M.; Haglind, F.; Asim, M.; Zeb Alvi, J. Recent Research Trends in Organic Rankine Cycle Technology: A Bibliometric Approach. *Renew. Sustain. Energy Rev.* **2018**, *81*, 552–562. [CrossRef]
31. Tartière, T.; Astolfi, M. A World Overview of the Organic Rankine Cycle Market. *Energy Procedia* **2017**, *129*, 2–9. [CrossRef]
32. Available online: https://www.turboden.com/products/2463/orc-system (accessed on 30 November 2021).
33. Morrone, P.; Algieri, A. Biomass Exploitation in Efficient ORC Systems. *Appl. Mech. Mater.* **2012**, *260–261*, 77–82. [CrossRef]
34. Schuster, A.; Karellas, S.; Kakaras, E.; Spliethoff, H. Energetic and Economic Investigation of Organic Rankine Cycle Applications. *Appl. Therm. Eng.* **2009**, *29*, 1809–1817. [CrossRef]
35. Zhai, H.; An, Q.; Shi, L.; Lemort, V.; Quoilin, S. Categorization and Analysis of Heat Sources for Organic Rankine Cycle Systems. *Renew. Sustain. Energy Rev.* **2016**, *64*, 790–805. [CrossRef]
36. Drescher, U.; Brüggemann, D. Fluid Selection for the Organic Rankine Cycle (ORC) in Biomass Power and Heat Plants. *Appl. Therm. Eng.* **2007**, *27*, 223–228. [CrossRef]
37. Ismail, H.; Aziz, A.A.; Rasih, R.A.; Jenal, N.; Michael, Z.; Roslan, A. Performance of Organic Rankine Cycle Using Biomass as Source of Fuel. *J. Adv. Res. Appl. Sci. Eng. Technol.* **2016**, *4*, 29–46.
38. Algieri, A. Comparative Investigation of the Performances of Subcritical and Transcritical Biomass-Fired ORC Systems for Micro-Scale CHP Applications. *Procedia Comput. Sci.* **2016**, *83*, 855–862. [CrossRef]
39. Pezzuolo, A.; Benato, A.; Stoppato, A.; Mirandola, A. Fluid Selection and Plant Configuration of an ORC-Biomass Fed System Generating Heat and/or Power. *Energy Procedia* **2016**, *101*, 822–829. [CrossRef]
40. Jang, Y.; Lee, J. Optimizations of the Organic Rankine Cycle-Based Domestic CHP Using Biomass Fuel. *Energy Convers. Manag.* **2018**, *160*, 31–47. [CrossRef]
41. Mikielewicz, D.; Mikielewicz, J. Criteria for Selection of Working Fluid in Low-Temperature ORC. *Chem. Process Eng.* **2016**, *37*, 429–440. [CrossRef]
42. Moharamian, A.; Soltani, S.; Rosen, M.A.; Mahmoudi, S.M.S.; Morosuk, T. A Comparative Thermoeconomic Evaluation of Three Biomass and Biomass-Natural Gas Fired Combined Cycles Using Organic Rankine Cycles. *J. Clean. Prod.* **2017**, *161*, 524–544. [CrossRef]
43. Fernández, F.J.; Prieto, M.M.; Suárez, I. Thermodynamic Analysis of High-Temperature Regenerative Organic Rankine Cycles Using Siloxanes as Working Fluids. *Energy* **2011**, *36*, 5239–5249. [CrossRef]
44. Méndez-Cruz, L.E.; Gutiérrez-Limón, M.Á.; Lugo-Méndez, H.; Lugo-Leyte, R.; Lopez-Arenas, T.; Sales-Cruz, M. Comparative Thermodynamic Analysis of the Performance of an Organic Rankine Cycle Using Different Working Fluids. *Energies* **2022**, *15*, 2588. [CrossRef]
45. Thurairaja, K.; Wijewardane, A.; Jayasekara, S.; Ranasinghe, C. Working Fluid Selection and Performance Evaluation of ORC. *Energy Procedia* **2019**, *156*, 244–248. [CrossRef]
46. Babatunde, A.F.; Sunday, O.O. A Review of Working Fluids for Organic Rankine Cycle (ORC) Applications. In Proceedings of the 2nd International Conference on Engineering for Sustainable World (ICESW 2018), Ota, Nigeria, 9–13 July 2018; Volume 413, p. 012019. [CrossRef]
47. Arjunan, P.; Gnana Muthu, J.H.; Somanasari Radha, S.L.; Suryan, A. Selection of Working Fluids for Solar Organic Rankine Cycle—A Review. *Int. J. Energy Res.* **2022**, 1–27. [CrossRef]
48. Imre, A.R.; Kustán, R.; Groniewsky, A. Thermodynamic Selection of the Optimal Working Fluid for Organic Rankine Cycles. *Energies* **2019**, *12*, 2028. [CrossRef]
49. Zhang, X.; Zhang, Y.; Cao, M.; Wang, J.; Wu, Y.; Ma, C. Working Fluid Selection for Organic Rankine Cycle Using Single-Screw Expander. *Energies* **2019**, *12*, 3197. [CrossRef]
50. Invernizzi, C.M.; Ayub, A.; Di Marcoberardino, G.; Iora, P. Pure and Hydrocarbon Binary Mixtures as Possible Alternatives Working Fluids to the Usual Organic Rankine Cycles Biomass Conversion Systems. *Energies* **2019**, *12*, 4140. [CrossRef]
51. Uusitalo, A.; Honkatukia, J.; Turunen-Saaresti, T.; Grönman, A. Thermodynamic Evaluation on the Effect of Working Fluid Type and Fluids Critical Properties on Design and Performance of Organic Rankine Cycles. *J. Clean. Prod.* **2018**, *188*, 253–263. [CrossRef]
52. Chen, H.; Goswami, D.Y.; Stefanakos, E.K. A Review of Thermodynamic Cycles and Working Fluids for the Conversion of Low-Grade Heat. *Renew. Sustain. Energy Rev.* **2010**, *14*, 3059–3067. [CrossRef]

53. Poling, B.E.; Prausnitz, J.M.; O'Connell, J.P. *The Properties of Gases and Liquids*; McGraw-Hill Professional: New York, NY, USA, 2000.
54. Calm, J.M.; Didion, D.A. Trade-Offs in Refrigerant Selections: Past, Present, and Future. *Int. J. Refrig.* **1998**, *21*, 308–321. [CrossRef]
55. Bell, I.H.; Wronski, J.; Quoilin, S.; Lemort, V. Pure and Pseudo-Pure Fluid Thermophysical Property Evaluation and the Open-Source Thermophysical Property Library CoolProp. *Ind. Eng. Chem. Res.* **2014**, *53*, 2498–2508. [CrossRef] [PubMed]
56. Chen, Q.; Xu, J.; Chen, H. A New Design Method for Organic Rankine Cycles with Constraint of Inlet and Outlet Heat Carrier Fluid Temperatures Coupling with the Heat Source. *Appl. Energy* **2012**, *98*, 562–573. [CrossRef]
57. Wang, J.; Yan, Z.; Wang, M.; Ma, S.; Dai, Y. Thermodynamic Analysis and Optimization of an (Organic Rankine Cycle) ORC Using Low Grade Heat Source. *Energy* **2013**, *49*, 356–365. [CrossRef]
58. Sarkar, J. A Novel Pinch Point Design Methodology Based Energy and Economic Analyses of Organic Rankine Cycle. *J. Energy Resour. Technol.* **2018**, *140*, 052004. [CrossRef]
59. Li, Y.-R.; Wang, J.-N.; Du, M.-T.; Wu, S.-Y.; Liu, C.; Xu, J.-L. Effect of Pinch Point Temperature Difference on Cost-Effective Performance of Organic Rankine Cycle: Effect of PPTD on Cost-Effective Performance of Organic Rankine Cycle. *Int. J. Energy Res.* **2013**, *37*, 1952–1962. [CrossRef]
60. Zhang, X.; He, M.; Wang, J. A New Method Used to Evaluate Organic Working Fluids. *Energy* **2014**, *67*, 363–369. [CrossRef]
61. Darvish, K.; Ehyaei, M.; Atabi, F.; Rosen, M. Selection of Optimum Working Fluid for Organic Rankine Cycles by Exergy and Exergy-Economic Analyses. *Sustainability* **2015**, *7*, 15362–15383. [CrossRef]